BTA/TG/12-04 **Salt Reserve Estimate for the Twenthe-Rijn concession**

May 2012 **M.C. Ensing**

Department of Geotechnology

Delft University of Technology

Title	:	Salt Reserve Estimate for the Twenthe-Rijn concession
Author(s)	:	M.C. Ensing
Date	:	May 2012
Professor(s)	:	Prof.dr. S.M. Luthi
Supervisor(s)	:	R.M. Groenenberg
TA Report number	:	BTA/TG/12-04

Postal Address : Section for Applied Geology
Department of Applied Earth Sciences
Delft University of Technology
P.O. Box 5028
The Netherlands
Telephone : (31) 15 2781328 (secretary)
Telefax : (31) 15 2781189

Preface

This study has been done during an internship of the author during July and August 2011 at the Mining Department of AkzoNobel Industrial Chemicals in Hengelo and is also submitted as his BSc. Project as part of the Bachelors programme in applied earth sciences at the Faculty of Civil Engineering and Geosciences of the Delft University of Technology.

This report is intended to increase the understanding of the steps to be taken when assessing the total reserves in a (bedded) salt body when using solution mining. It deals with the definitions and the mathematics one might encounter in such an endeavour.

I want to thank my supervisor at AkzoNobel, dr. R.M. Groenenberg, for his supporting of my internship, his suggestions, his patience with me and for the discussions we had during my time there. I also want to thank prof. dr. S.M. Luthi, my supervisor at the TU Delft for helping me in submitting this report as my BSc. Thesis and examining my work.
At AkzoNobel I also received a lot of help and good suggestions from the team at the Mining Department and I want them to receive my thanks as well.

This is the third edition of this report, after initial comments from dr. Groenenberg followed by recommendations made by prof. Luthi. Future revisions may appear as it is further reviewed by my supervisors.

Michiel Ensing
Delft, April 2012

Table of Contents

Summary

AkzoNobel has been producing salt from solution-mined brine since 1919. Production in the Hengelo area started in 1933, and is still ongoing today. Because at some point in time the mineable salt will all be mined and preparations for extension of the concession will need to be made, it is important to know the remaining amount of salt in the Hengelo area. To date no singular method for estimation of these reserves has been adopted. This leaves room for the development of a local method. It was chosen to develop this method in accordance with international standards. Due to its worldwide influence and being recognised by the Amsterdam Stock Exchange that AkzoNobel is registered on, it was opted to use the code of the Joint Ore Reserves Committee (JORC) of the Australasian Institute of Mining and Metallurgy (AusIMM).

The geology of the Hengelo area was modelled using a modified version of the ordinary Kriging algorithm to take into account the presence of faults. Kriging was used because it also provides an estimate of uncertainty in the horizons that are modelled. To factor in the uncertainty about the continuity of the salt body, the resources in three areas were calculated: the area was investigated as a whole, and two sub-areas were investigated separately:

- Sub-area 1 is the area within 500m distance of any measurement in the area.
- Sub-area 2 is the area for which the geology was previously studied in great detail by GeoWulf Laboratories[5]. This area is essentially the area in-between the different measurements.

The modelled horizons and their uncertainty values were then used in a Monte Carlo simulation, yielding cumulative probability distributions for the estimated amount of salt in the three scenarios. The total amount of salt was also calculated deterministically, meaning all calculations were performed using expected values. This produced the same values as the expectations of the probabilistic approach. It was decided that the probabilistic approach of the total area produced an over-optimistic value of the total Resource, and to only use the expected values of the three areas to distinguish between Inferred, Indicated and Measured Resources.

Reserves were estimated for three scenarios:

1. Salt has been produced in the past in this area using a no longer used leaching strategy that results in large caverns with multiple wells. What would be the Salt Produced if the same locations had been chosen to produce salt using the modern Single Completion Cavern design? And what would be the historical recovery?
2. Assuming no production had taken place in the past, what would be the total Salt Reserve if the field would be developed now?
3. What is the Salt Reserve left in the area?

It was found that the recovery percentages per cavern as asked for in scenario 1 were so widespread that no conclusive numbers could be given.

The cavern lay-out throughout the area in scenarios 2 and 3 was not optimized, but because the overall estimation process was conservative the numbers could still be used as minimal values in future evaluations of the area. The results of scenario 3 are given in the table below.

Mineral Resource		Salt Reserve	
Inferred	117 Mt	-	-
Indicated	159 Mt	Probable	13.6 Mt
Measured	3.8 Mt	Proven	3.8 Mt

1. Introduction

AkzoNobel and its predecessors have been mining salt in the area around Hengelo in the eastern part of the Netherlands since 1919. At first mining was done in the Buurse concession south of Enschede, but with the completion of the Twente Canal in 1933, it was more favourable to continue production in the Twenthe-Rijn concession around Hengelo. The salt is mined by solution mining. In solution mining, salt is produced from the subsurface by pumping fresh water downwards into a salt layer. At depth, the salt dissolves into the fresh water, thus creating a hollow space or cavern filled with brine that can be produced. Salt is recovered from the saturated, purified brine by recrystallization in a vacuum pan salt refinery in exceptionally pure form for use in food, medicine and chlor-alkali producers.

Since salt is widely present in the area, there was never great concern about the amount of salt available for production. Only since 1992, studies have been done to investigate the total salt reserves. At that time subsidence issues and the formation of a sinkhole led to the development of new mining practices. These practices limited the amount of salt that could be mined from an area, so knowing the amount of salt present in the area became more critical. Several studies regarding the amount of reserves have so far been done by TNO-NITG, Oranjewoud and MWH. All these studies have been done to provide an estimate of the remaining reserves in (a part of) the Twenthe-Rijn concession. Unfortunately these studies all differ in their approach and none are compliant with international standards.
To be able to value these reserves as assets, international reporting standards as specified in different professional codes have to be adhered to. The code that is internationally most widely accepted, including at the Amsterdam Stock Exchange (NYSE Euronext) that AkzoNobel is registered on, is the Australasian JORC Code.

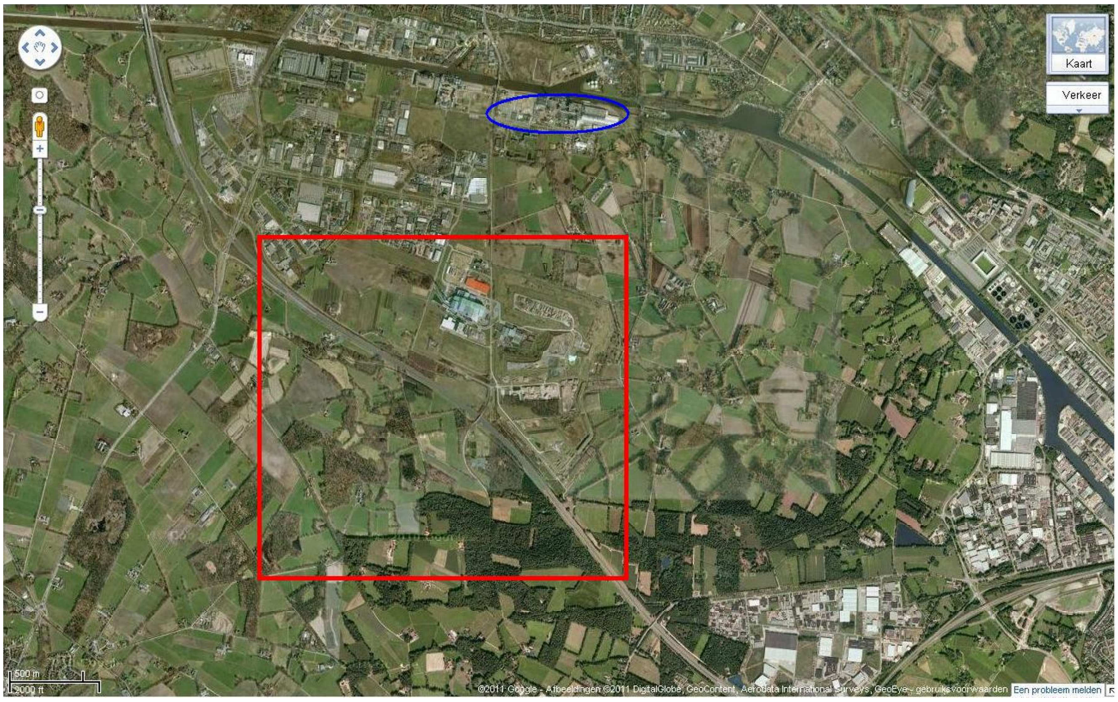

Figure 1.1: investigated area (outlined in red) on a satellite image. The location of the plant is indicated by the blue oval. To the right of the image lies the city of Enschede. To the top the city of Hengelo is just visible.

The objective of this study is to develop a procedure to estimate the salt resource and reserve that complies with the JORC Code. For this purpose, a geological model must be constructed and the guidelines in JORC Code must be translated into a method that is applicable to solution mining of salt in the Hengelo area.

The area that has been investigated is part of the Twenthe-Rijn concession and measures 2.5 km * 2.5 km = 6.25 km^2. The coordinates of the northwest corner are (249.200, 473.200) and those of the southeast corner are (251.700, 470.700) in the 'Rijksdriehoekscoördinaten' (Dutch State coordinate) system. The area is outlined on a satellite image in Figure 1.1.

2. Geology

In this chapter, a description is given of the geology of the Hengelo concession area. First the geologic setting of the region during the Triassic and Jurassic is reviewed when the salt layers (Main Röt Evaporite) were deposited. Next, the stratigraphy is described. Finally the salt layers of the Main Röt Evaporite are described in more detail.

2.1 Geologic Setting

Triassic (based entirely on Geluk, 2007[1])

At the start of the Triassic period, North-West Europe was located in a large continental basin that had been formed in Permian times, during the start of the break-up of the super-continent Pangea. This basin stretched from present-day England and the North Sea in the west to Poland and Lithuania in the east. In the Early Triassic, sediments that were deposited in the basin consisted mainly of clastics that originated mainly from the Variscan mountain ranges, such as the London-Brabant Massif that lay to the south. Parallel to the further break-up of Pangea, large scale extensional faulting took place in the region, leading to the formation of a number of smaller depo-centers. Rifting took place in several phases. The first one, the Hardegsen phase, marked the transition between the Early Triassic and the Middle Triassic. During this phase, a connection with the Tethys Sea to the south was formed in southern Germany, allowing the inflow of sea-water. During brief interruptions of this connection, due to local uplift, the evaporites that form the Main Röt Evaporite were deposited. For a map of the present day distribution of the Röt, see Figure 2.1 In a later stage of transgression, the connection was reestablished and the basin became of a more marine nature. During this time the Muschelkalk Formation was deposited, which consists mainly of carbonates. Rifting of the basement in what is known as the Early Kimmerian Rifting Phase caused an activation of the Zechstein salt layers, leading to large scale halokinesis in the northern Netherlands. At the same time the main source of sediment supply moved toward Fennoscandia, leading to widespread deposition of claystones alternating with small beds of evaporites.

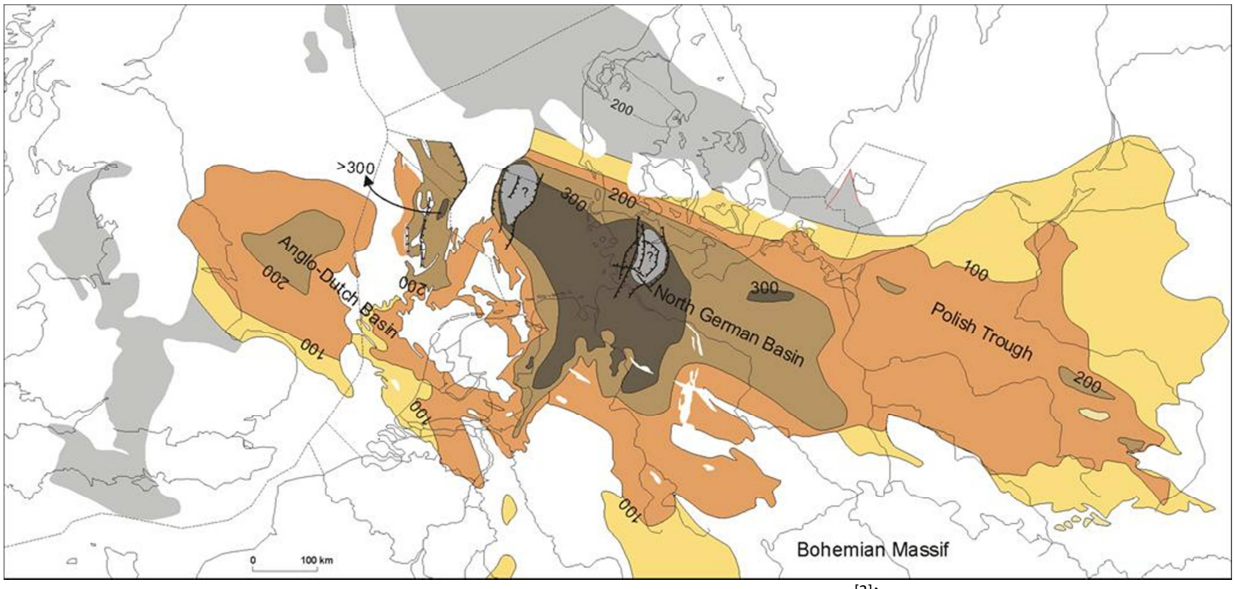

Figure 2.1: present day distribution and isopach map of the Röt Fm. (Geluk, 2007[2])

Jurassic (based entirely on Wong, 2007.[3])

The Jurassic was characterized by continuation of the break-up of Pangea. During this period there were two phases of extension, the Middle Kimmerian and the Late Kimmerian. In between these phases were times of thermal subsidence. During the Jurassic, deposition of sediments happened mainly in the different rift-basins that were formed in the Kimmerian rifting phases. The three major systems were (see also Figure 2.2)

- A N-S striking system that stretched from the Dutch Central Graben in the present-day North Sea to the Vlieland Basin.
- The Lower Saxony Basin, which had a E-W strike.
- A large NW-SE striking system, which incorporated the Broad Fourteens, West Netherlands and Central Netherlands Basins, as well as the Roer Valley Graben.

In between these basins lay highs where between the Early and Middle Kimmerian phases, sedimentation still took place. However, when the Middle Kimmerian phase was started due to thermal uplift of the North Sea Dome in the central North Sea, these areas became dry, and most Early Jurassic sediments were eroded. In between the Middle and Late Kimmerian phases, a southward transgression took place, gradually resubmerging the highs.

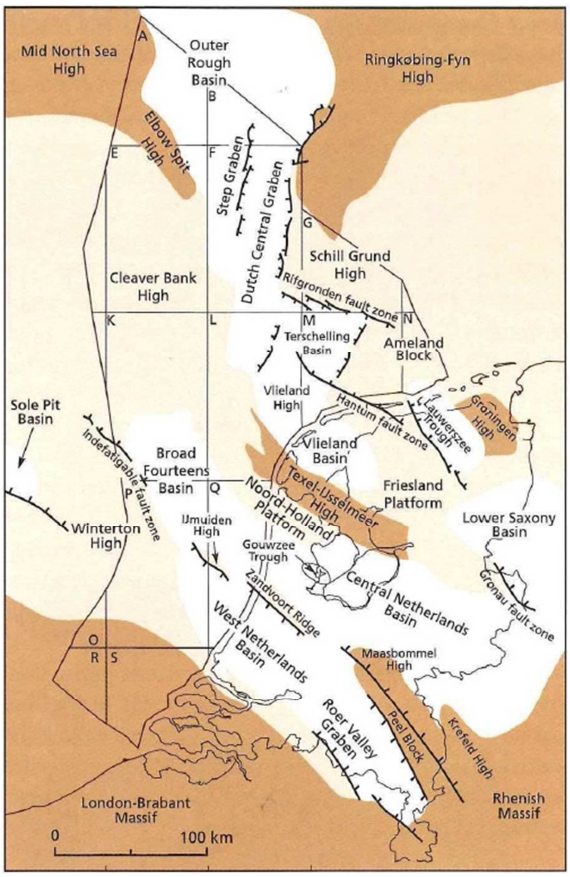

Figure 2.2: map of Late Jurassic and Early Cretaceous structures (Wong, 2007[3])

2.2 Lithostratigraphy

The stratigraphy of the area was studied in great detail by GEOWULF Laboratories in 2008[4]. The information in this part is based almost entirely upon their work.

At the base of the studied stratigraphic interval lies the Solling Formation, which consists mainly of claystone and has a sandstone at its base.

The Main Röt Evaporite (MRE) overlies the Solling Formation. It is the evaporitic section of the lower succession of evaporite and claystone as mentioned in the previous section. The MRE is subdivided into 5 lithological units (A-E), of which the lower four (A-D) consist mostly of halite with some intermixed anhydrite and clay. The salt has a grey colour, which reddens towards the top of the MRE indicating an increasing presence of hematite. Each halite section has a non-halite section at its base. For units A-D these are anhydrite, dolomite (2x) and claystone respectively. These will be referred to as 'rock benches' corresponding to the overlying salt unit.

Units A and C are the main salt layers that are being mined in the Hengelo operation. Units B and D are of considerably smaller thickness. Where salts A and C are usually each around 20

meters thick, salt B and D are only some 3 meters thick each. Unit D is also locally absent in some areas of the Twenthe-Rijn concession.

Directly overlying the MRE is the Muschelkalk Formation, consisting mainly of limestone and marl alterations, with a thin evaporitic alteration also being present.

The Keuper Formation, which stratigraphically succeeds the Muschelkalk, is absent in the region due to Early Kimmerian erosion. Middle and Late Kimmerian erosion also caused most of the Jurassic Altena Group to be regionally absent. Only the Sleen Formation, which is actually from Triassic times[1], remains. It consists of a base of grey, marine claystones, which are overlain by brown, sandier claystones[4].

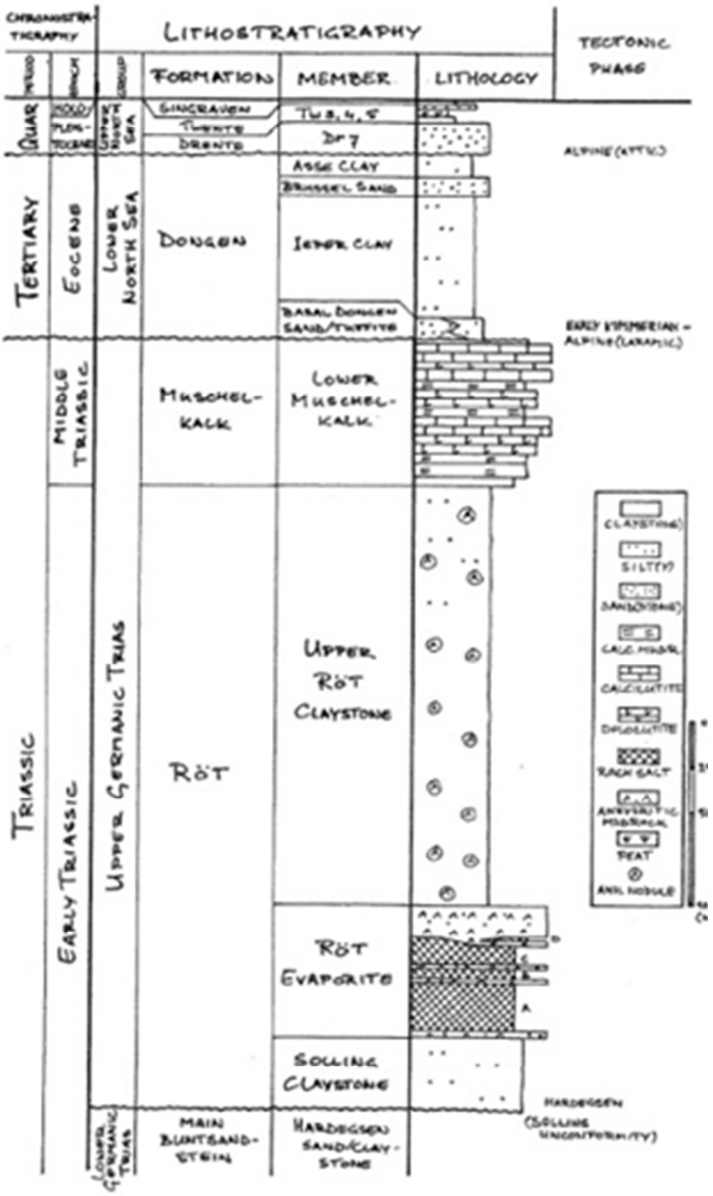

Figure 2.3: Stratigraphic column of the studied area (Van Lange, 1994[7])

Overlying the Triassic are only deposits from Cenozoic times. The formations from the Cretaceous and Jurassic are not present in the area. As they have been found in surrounding areas, it is assumed that sedimentation took place in the studied area as well. The Cenozoic sediments date from Eocene-Pleistocene times. They consist of a varying composition of clays and quartz and glauconite sands, and are generally unconsolidated. Because of the similarities in depositional environments, these sediments –which date from Eocene to Pleistocene times – have been grouped in the North Sea Supergroup.

3. Mining Method & Geotechnical aspects

3.1 Mining Method

This chapter contains a description of the mining method used in the production of salt in the Hengelo area. The process may differ from those in other locations. The description is based on the 'Hengelo Uitloog Techniek 2011' document [6], which outlines the 'Good Salt Mining Practice' mining methods used in Hengelo.

General description

In the Hengelo area, salt is produced using a solution mining method. This means that water is pumped through a borehole into the salt formations to dissolve ('leach') the salt, forming a saturated brine. This brine is then pumped back up to the surface. The leaching of the salt leads to the formation of a cavern in the salt formation. These caverns can be as large as a football stadium (W. Paar, pers. comm.). The upward growth of the cavern is controlled using a 'blanket' of a fluid or compressed gas that is lighter than water and does not dissolve the overlying salt. A schematization of the process is provided in figure 3.1.

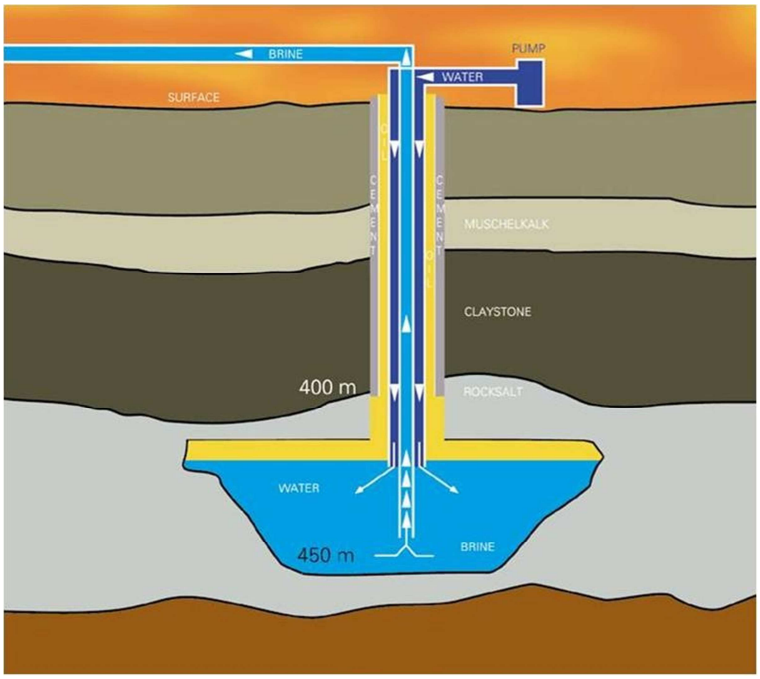

Figure 3.1: schematization of the leaching process in a Single Completion Cavern (SCC).

In the plant the brine is first purified, removing any dissolved salts other than NaCl. After that, the water is removed from the brine through evaporation. This is accomplished by adding heat to the brine, and subsequently lowering the pressure, allowing the water to evaporate.

Cavern development

There are two types of caverns in the Hengelo area that both have the general shape of a pancake – meaning the width is much larger than the thickness and they have a more or less circular shape. The older type of cavern is called a "Multiple Completion Cavern" (MCC), because it is developed from three smaller caverns (with one well each) that are later connected to form a large cavern with an elongated geometry. The new type, which is the only one still being developed, uses only a single well and is called a Single Completion Cavern (SCC). This change in design has significantly shortened the time needed to bring a cavern into full production. Where the old caverns needed 8 to 10 years, the new ones only need around 14 months to start producing saturated brine. Since MCC's are no longer being developed, it shall not be discussed further in this paragraph.

An SCC typically has a diameter of 120 meters and a height of between 20 and 30 meters.After completion, the well consists of a cemented casing in which two tubings are installed. The

annular space between the casing and the outer tubing is filled with a blanket fluid or gas – commonly diesel fuel. The annular space between the two tubings is used for water injection, and the inner tubing is used to produce brine (see Figure 3.1). The sump phase of the cavern, which lasts 14 months, is then started. In the sump phase, an 'undercut' with a diameter of 80 meters is developed in the salt layer.

Production

Brine can be produced (leaching phase) from an SCC for a period of about 15-20 years, depending on the production rate, the thickness of the salt layer and the geomechanical properties of the subsurface in the immediate vicinity of the cavern.

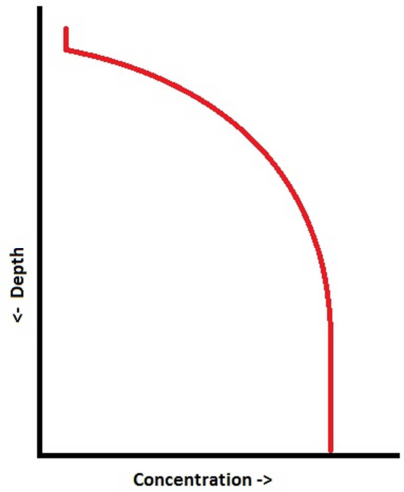

Figure 3.2: schematization of the brine concentration versus the depth inside a cavern

A basic principle of the leaching process is that the flow of water into a cavern is comparable to the flow of a garden hose into a swimming pool. The amount of water pumped in is negligible compared to the overall volume of water in the cavern. The body of water therefore hardly 'notices' the flow, and can be said to be at rest. This means that the concentration of the brine is equal at any one point in a horizontal plane. The only difference in concentration is along the vertical axis, because of the difference in density between water and saturated brine. This is also the reason why water is injected at the top, and brine extracted from the bottom. The concentration profile indicates that if the roof would not be shielded by a blanket, the leaching there would take place at a greater speed than at the sides, as the concentration of the brine is lower near the roof. For a schematization of the concentration in a cavern, see Figure 3.2.

Abandonment

Current regulations require that a concession be properly abandoned once production has ceased, which is not yet the case for the Hengelo concession area. At end of production, caverns remain filled with brine, which acts as a stabilizing agent. Boreholes are sealed off with a cement plug, and boreholes and cavern continue to be monitored for subsidence.

3.2 Geotechnical aspects

The main geohazards associated with solution mining are surface subsidence and the formation of sinkholes[6]. To prevent sinkholes from forming and to limit any subsidence, caverns have to be limited in size and pillars of salt have to be left in between the caverns. The information in these paragraphs comes from the 'Hengelo Uitloog Techniek'[6] document and from Van Lange, 1994[7].

Sinkholes

Sinkholes are formed when a cavern migrates to the surface, i.e. when the roof of the cavern collapses. For the formation of sinkholes, the height of the cavern was found to be of large influence, whereas the width of the cavern has very little influence [7]. It was found that when the compacted overburden – everything between the roof of the cavern and the Base Tertiary –

collapsed, the accompanying 'bulking' of the total overburden volume could fill the underlying void up to a certain height [7]. This height was then defined as the maximum height for inherently stable caverns, and can be calculated using formula (1).

$$TCAV = \{BCAV + (BF - 1) * (BT + 40)\}/BF \quad (1)$$

With:

TCAV = Minimum depth of top of cavern for intrinsically stable cavern
BCAV = Depth of bottom of cavern
BT = Depth of Base Tertiary
BF = Bulking factor
All numbers are taken positive

To ensure stability over longer times – and greater recompaction – a relatively low bulking factor of 1.11 was assumed. As an added level of safety, instead of the Base Tertiary an imaginary line lying 40 meters lower was taken as a reference, explaining the +40 in (1). Additionally, the old requirement of a stability roof in the salt was maintained. To reduce the chance of roof collapse, a safety roof of 5 meters in salt layer C is to be maintained at all times. This means that that:

$$TCAV \geq TZC + 5 \quad (2)$$

With all numbers taken positive and:

TZC = Top of Salt C

The measures described above are part of the Good Salt Mining Practice (GSMP), which was developed after a sinkhole formed in Hengelo in 1991 to prevent against the future formation of sinkholes. To this day no other sinkhole has formed.

Subsidence

Surface subsidence is caused by the viscoplastic nature of salt[7]. This means that the salt surrounding the cavern behaves more or less as a fluid when pressurized and thus slowly 'creeps' back into the void, thereby closing it. To minimize the surface subsidence, the pressure acting on the roof and floor of the cavern has to be diverted along the salt pillars in between the caverns[7]. This places limits on the lateral extent of the caverns, and requires pillars of adequate size. To limit the surface subsidence to 0.5 mm/yr, the width of the cavern is limited to 120 meters[6]. The caverns are also placed in rows, with 150 meters between the caverns in a row and 450 meters between two rows, all measured from the center of each cavern[6].

4. Geological modelling

To estimate the amount of salt in place and to discover if the salt can be extracted economically, we need to form an idea of how the salt is situated in the subsurface and quantify the geometry of the salt body in a grid. The specific geological features this report focuses on are the boundaries between different formations. For this we use the data gathered from boreholes in the region. If seismic data were available this could also be used. For interpolating grid values an adaptation of ordinary kriging was used.

The data

As mentioned, the data comes from gamma-ray logs and so-called 'boorboeken' of the boreholes in the region. A boorboek contains information about the nature of the cuttings related to drilling depth. All gamma-ray logs were interpreted by GeoWulf Laboratories[5]. There are 206 boreholes in the region, of which 9 did not provide any data and 54 only provided data about the Base Tertiary boundary. A visualisation of the data locations is given in figure 4.1. All data values were calculated relative to mean sea level (NAP). The raw data can be found in appendix A.

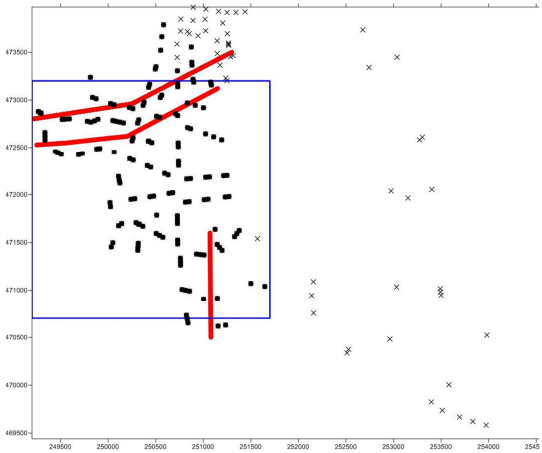

Figure 4.1: distribution of the data points in plan view. The blue box marks the modeled area, the red lines mark the most prominent fault lines. Crosses are data points with only Tertiary data.

Kriging

To construct a grid with depth values for the various formation boundaries, an interpolation technique has to be applied. As we want to be able to quantify the uncertainty of the values later on, the technique used has to be able to quantify that as well. This condition favours a technique common in exploration geology, called kriging.

In kriging, the data is used not only to construct the interpolated values given a set of weights, but is also used to calculate the weight given to each datum[8]. This is done by first constructing a so-called semi-variogram, where the semivariance –which is half of the squared difference– is plotted against the distance between two values. This then provides a very spiky line, through which we can draw a model variogram. These model variograms are based upon standard formulas which will aid us later in the process. For an example of sample variogram and 2 models drawn through it, see Figure 4.3.

A model variogram has three important parameters: the Nugget, the Sill and the Range. (see Figure 4.2)The Nugget is the semivariance at distance 0. This would normally be 0, but if there is an uncertainty in the data this can be modelled here. The Sill is the maximum semivariance of the variogram. Since after a certain distance there is no further effect of the data on the interpolation point, it is convenient to assign all this data the same semivariance value.

The Range is the distance after which the variogram loses its effect and the Sill value is assigned.

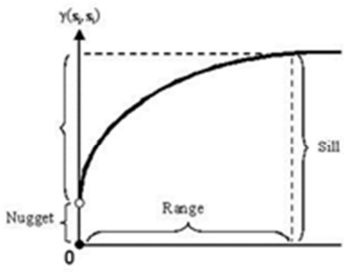

Figure 4.2: visualisation of the three parameters of a model variogram.

For kriging to work, we first need to make sure that the data is stationary[8,9], meaning that the expectation of the modelled variable is constant in space. In our case, when working with the depth of a surface, that is not necessarily a given. Therefore we first need to estimate the regional trend, called the *Drift* and subtract it from our data[9]. The results, called the *Residuals* can then be assumed to be stationary[9]. We can then model the Residuals using kriging, and later add the modelled Drift to these residuals. Since geological examination has shown the salt body to have a more or less linear dipping trend[5], a *least squares approximation* with 2 variables, x and y, was done for each surface. This results in a dipping plane, just as the geology indicates.

After the variogram has been modelled using the Residuals, kriging can be performed on the Residuals. For this we construct a matrix C and a vector D for each point. The matrix C consists of the semivariances between all points. The vector D consists of the semivariances between the interpolation point and all other points[8].
A feature of ordinary kriging is to guarantee that the weights λ1, λ2,…, λI add up to exactly one[8]. This guarantees that all interpolated values lie between the minimum and maximum data point. For this we also add a row to the matrix C that consists of a 1 for every λ. The system we now have is over defined, so a column of ones is added[8]. The bottom right variable of the matrix is 0, as this new weight –which we will call μ– should have no effect on the range of the interpolated value. All in all this leads to equation (3) displayed below, where γ_{ij} is the semivariance between point i and j.

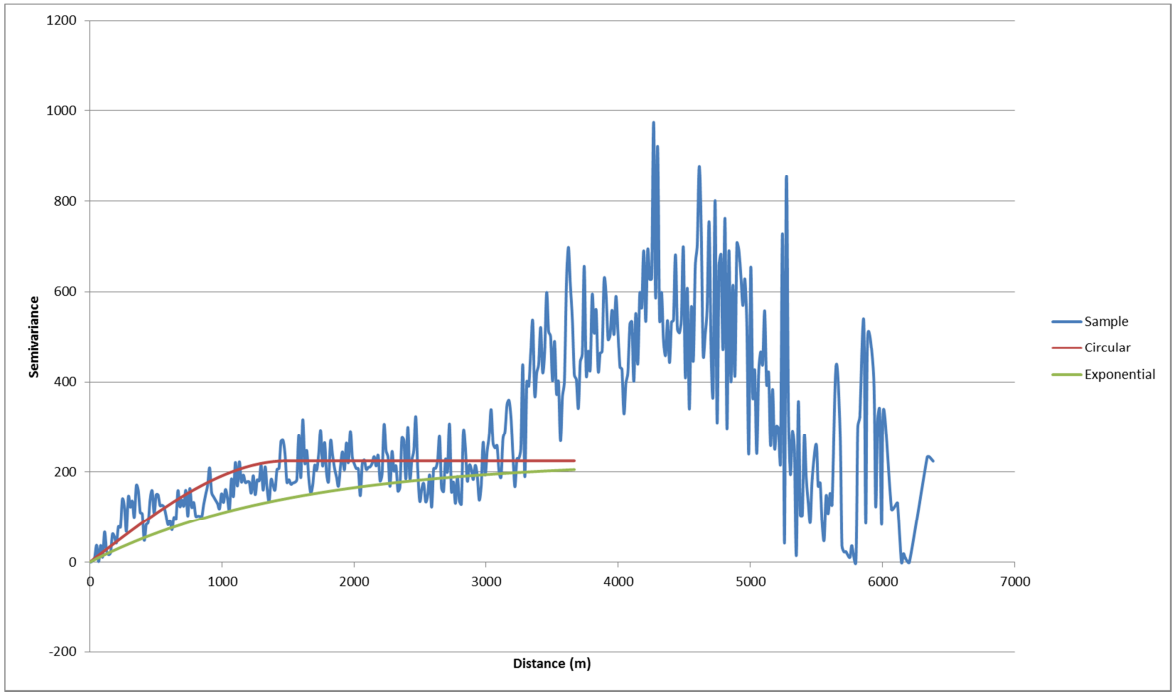

Figure 4.3: a sample variogram with 2 models drawn through it. The circular model clearly displays the Sill and Range. The shown exponential model has the same parameters as the circular, but due to its exponential nature the Sill act as an asymptote. Clearly visible is that the sample variogram continues well beyond the Range. But because it has already stabilized after 1500 m it was deemed that further modelling would unnecessarily complicate both the variogram modelling and the kriging process.

$$\begin{pmatrix} \gamma_{11} & . & . & \gamma_{1I} & -1 \\ . & . & . & . & . \\ . & . & . & . & . \\ \gamma_{I1} & . & . & \gamma_{II} & -1 \\ 1 & . & . & . & 0 \end{pmatrix} \begin{pmatrix} \lambda_1 \\ . \\ . \\ \lambda_I \\ \mu \end{pmatrix} = \begin{pmatrix} \gamma_{01} \\ . \\ . \\ \gamma_{0I} \\ 1 \end{pmatrix} \quad (3)$$

When this system has been solved, the weights λ1, λ2,….λI are used to calculate the interpolated value. This is done according to (4), where Z is the kriged variable, and point A is the interpolation point.

$$Z_A = \sum_{i=1}^{I} \lambda_i Z_i \quad (4)$$

The 'bonus' of kriging is that we can now also calculate the kriging variance. This is done according to (5), where γ is the semivariance and σ_A^2 is the kriging variance.

$$\sigma_A^2 = (\sum_{i=1}^{I} \lambda_i \gamma_{iA}) - \mu \quad (5)$$

Adapting the kriging method

The problem with kriging in most commercial software such as Surfer 10, which was available during the project, is that they provide a kriging function that cannot account for the presence of faults. Faults have a detrimental effect on any surface depth estimate, as the depth on one side of the fault differs from that on the other side. At the same time the distance between the two points is very small. This means that in the kriging process they will heavily influence each other, while actually being poorly related.

To counteract this effect, an algorithm was developed that checks if the 'line of sight' between the interpolation point and a datum crosses a fault an uneven number of times (if the same fault is crossed twice, the two point are actually on the same side of the fault). If so, the datum is discarded for the evaluation of that particular interpolation point.

The faults as indicated by GeoWulf[5] are entered into the algorithm in linear sections. The algorithm constructs the equations of all fault sections in the area. It then constructs the equation of the line of sight between the grid point and the datum. If a fault section intersects between the grid point and the datum, it is considered an intersection. If the total amount of intersections of one fault (all corresponding sections combined) is uneven, the two points are considered unrelated.

This algorithm is run for all data at each grid point. The remaining subset of the original dataset is then used for the kriging process. As faults also have an influence on the regional trend between fault lines, the regional trend –or Drift- is re-evaluated for this particular data subset. The Residuals are then kriged using (3) and (4) and the Drift is added again. This gives the interpolated value for the depth of a surface at that grid point. Equation (5) also holds for this subset and gives the kriging variance.

Results

The process described above is repeated for every point in a 101 x 101 grid, eventually providing enough data to plot surface maps and uncertainty maps. This was done for the surfaces *Base MRE*¸ *Top Salt C* and *Base Tertiary*, producing figures 4.4 through 4.9. These were chosen because they have the largest data amounts and are most important for later calculations (see also formulae (1) and (2). The variogram parameters used for different surfaces can be found in appendix B. All axis markers are in the Dutch State Coordinate System.

Discussion

Kriging is, as are all mathematical applications in geology, far from perfect. For example, kriging does not take geological considerations into account, but only considers the raw data. With the adaptations to the standard kriging process, which normally involves only inserting the raw data into a semivariogram and solving the equations (3), (4) and (5), the aim was to focus the data toward known aspects of the geology, such as linear dip and presence of faults. This process has also slightly corrupted the mathematics behind kriging. As we have constructed a separate data subset for every grid point, it would be necessary to construct a sample and model variogram for every grid point. But, as constructing a model variogram is done best using the human eye, it is in the interest of time that only the variograms for the entire dataset of each surface are constructed. It can be argued that, because the data that was discarded in the creation of the subsets creates larger variances at relatively small distances, the variogram is overestimated, thus implying that the model variogram gives a higher variance than the actual variance that can be expected at a certain distance. This would mean that the estimation of the surface depth might differ slightly from that calculated from a separate variogram for each grid point. However, because the variance in this case would also be smaller, the larger variance obtained in the used procedure reflects this added uncertainty.

A striking feature in figure 4.3 is that, after ~3000m separation the sample semivariance grows again to eventually stabilize around 550, even though it had stabilized around 220 already after 1500m separation. This could be explained by the aforementioned flaw in the process of variogram modelling. This increase could be the result of comparing two very different data sets, that are separated by a fault. Because data on opposing sides of faults could not be taken out in the process, we end up with that data corrupting our sample variogram. The reason it mainly shows at larger separation distances is that only two points from the different data sets are separated at such large values.

When we look at the produced surface images (see figures 4.4, 4.6 and 4.8), the regional trends become immediately clear. In fact, they are similar to the trends on the maps produced by GeoWulf. The produced contours are actually even more continuous than the GeoWulf ones, possibly owing to a scale difference. The fault zones clearly show artefacts of the Kriging process. At grid points with few or no relatable data points at all, the values tend to spike. It is therefore recommended to discard the grid points adjacent to the fault lines, so as to not corrupt further models.

More artefacts, but more subtle are the curved contour lines in areas where there is little data available, best visible in the bottom left corner of Figure 4.4. This is due to the fault in the bottom right corner acting as a shield, shielding the grid points to the west of this fault from the grid points to the west and northwest of this fault. The Drift component of the grid values to the

west are therefore affected and the regionally observed drift will change toward the south. With more data points in the southwest this effect would be mitigated, as those data points would contribute to a more realistic representation of the geology. Currently the data points toward the northeast have a relatively large impact on the values, which is clearly visible. Also in Figure 4.4 in the bottom left corner, at the far bottom, jagged edges are clearly visible. This is the same phenomenon as with the fault lines, but this time the exclusion of data points is due to the range of the variogram. Furthermore, there is Top Salt C specifically, which in the northwest corner exhibits the effect of a fault line. Here there is clearly not enough data available to do kriging, so the Drift component is most important for the estimated value. With a small amount of data, one outlier –which could have been realistic, had there been more data– can completely change the Drift formula, to produce the unrealistic image presented. This area, being small, will therefore be completely discarded in further modelling.

When looking at the uncertainty maps, the locations of the boreholes are clearly visible, because that is where the depth value is actually measured, and therefore uncertainty approaches zero. Furthermore, as soon as a grid point lies outside the data area the uncertainty increases significantly. After that, the increase of uncertainty decreases with distance from the nearest datum, probably due to the shape of the variogram (circular and exponential models were used, leading to a smaller increase in variance with distance). This means that the method applied so far is useful only in the area between data points. This is to be expected because Kriging is an *interpolation* method, rather than an *extrapolation* method.

Away from edges and fault lines, the surfaces produced aren't spectacular, also partly due to the fact that most local variations lie below the resolution. In Chapter 6, the trends in the thickness of the MRE are investigated, which are obtained by taking the difference in depth between the top and bottom of the MRE.

On the other hand the surface and uncertainty maps do provide an insight in the applicability of the method. It can clearly be shown that the main limitation of the method is the amount of available data. The spatial distribution of data points also contributes to the uncertainty values, however here it is also the larger concentration of data that give the best results. For best results, an even distribution of data over the entire area is desirable.

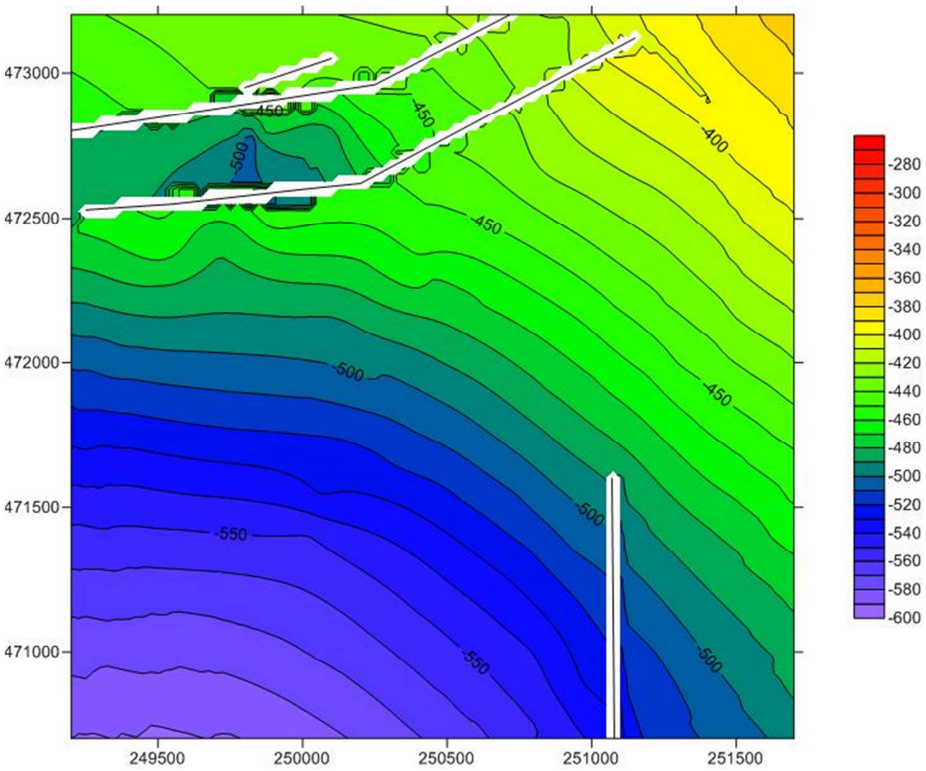

Figure 4.4: Base Main Röt Evaporite in meters below sea level.

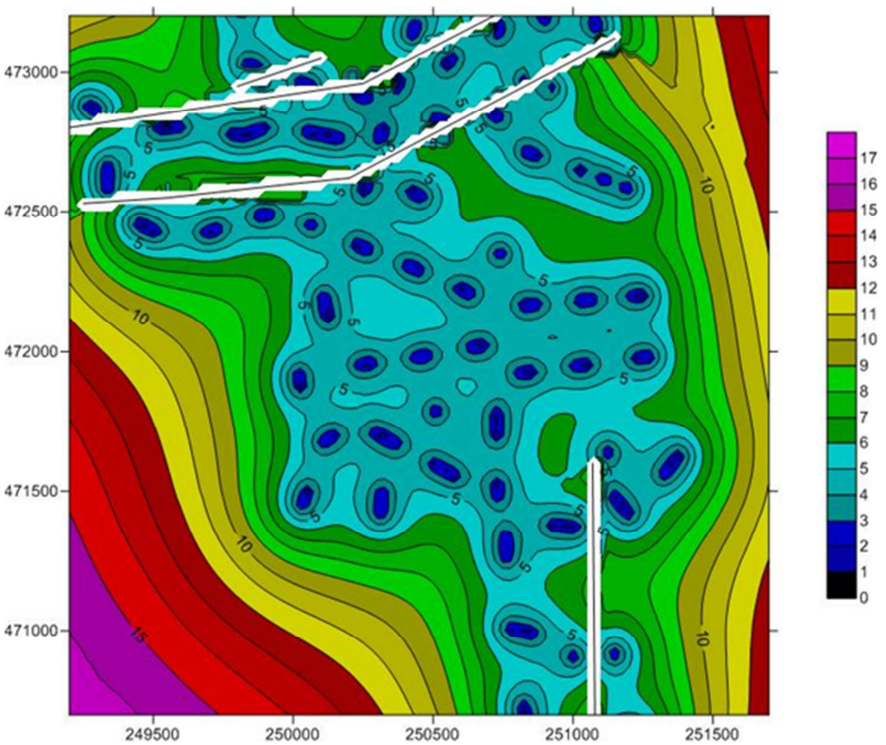

Figure 4.5: Base Main Röt Evaporite uncertainty map, displayed is the standard deviation σ (in meters), which is defined as the square root of the Kriging variance.

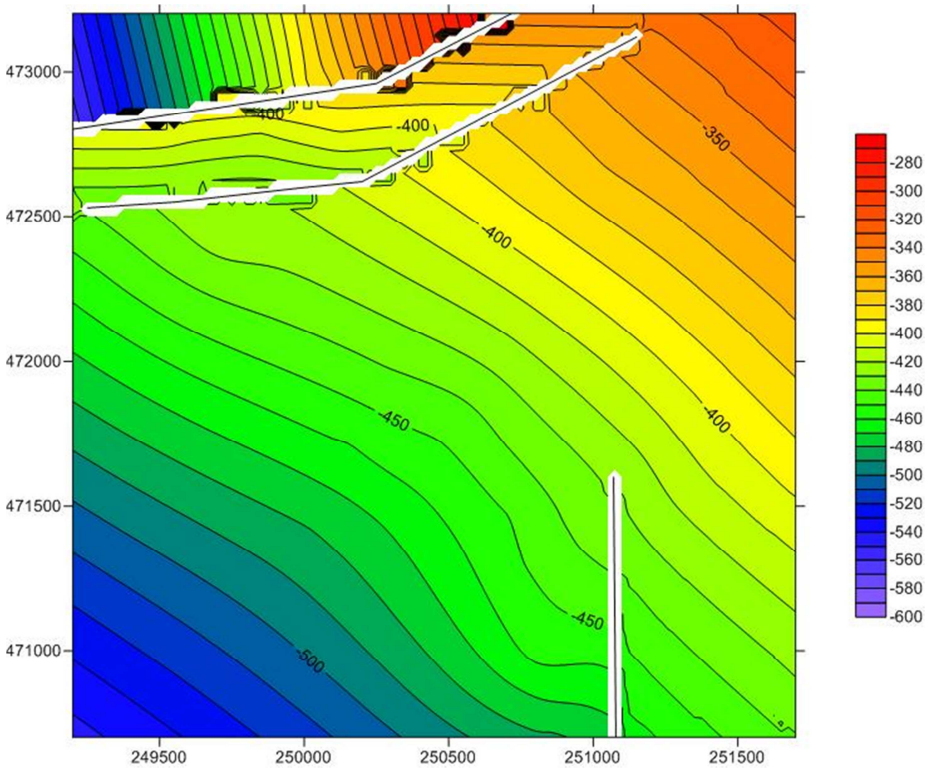

Figure 4.6: Top of Salt C in meters below sea level.

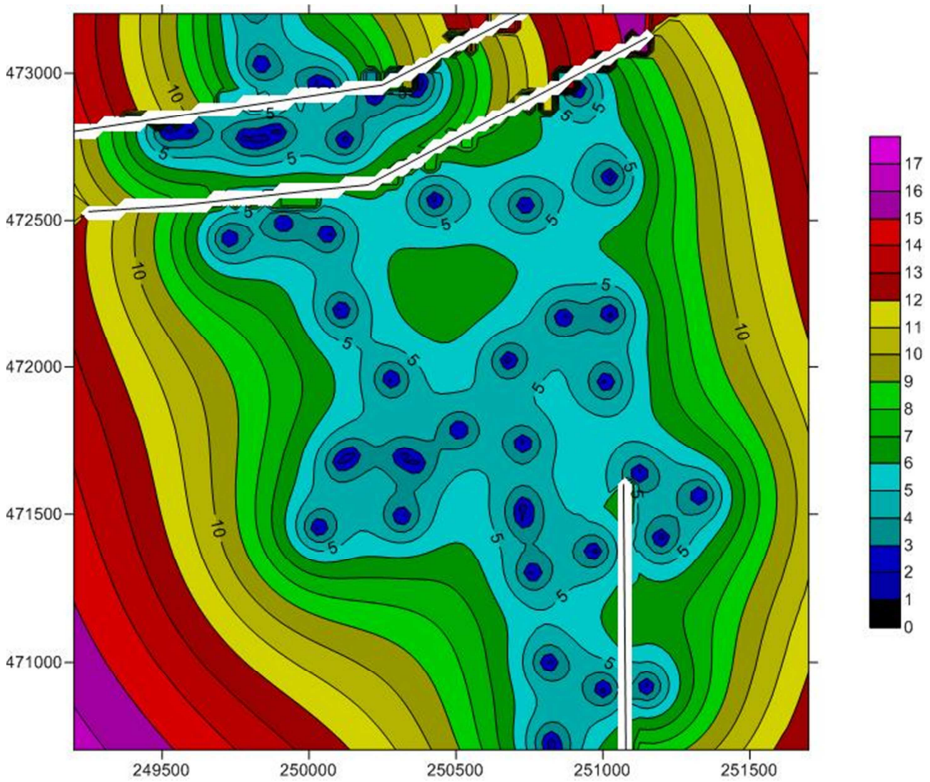

Figure 4.7: Top of Salt C uncertainty map, displayed is the standard deviation σ (in meters), which is defined as the square root of the Kriging variance.

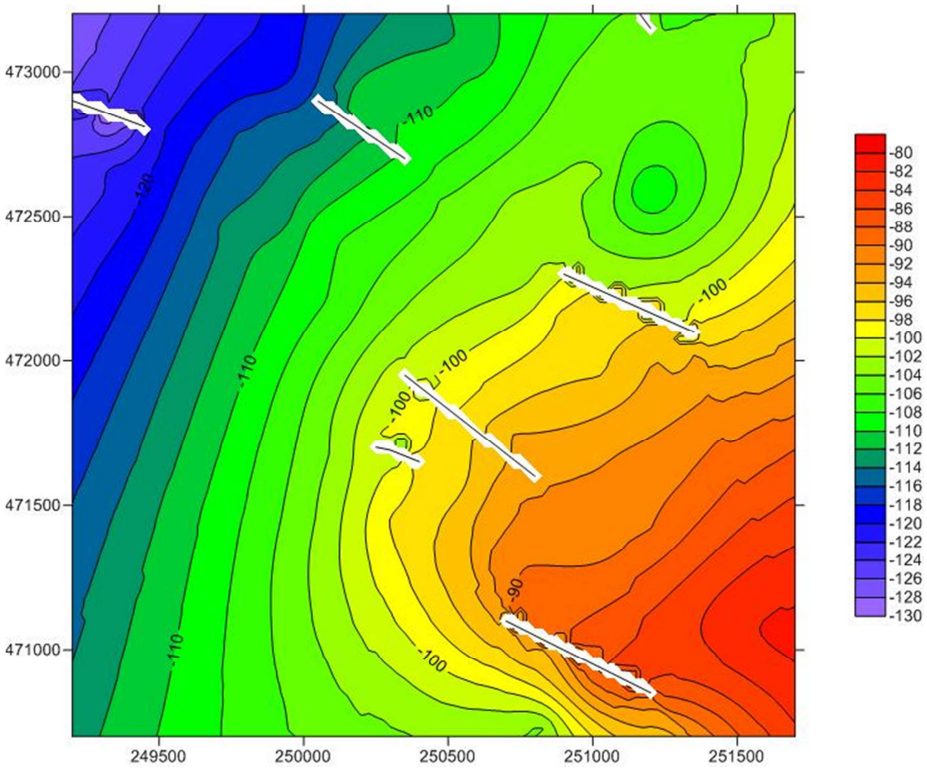

Fig 4.8: Base Tertiary in meters below sea level.

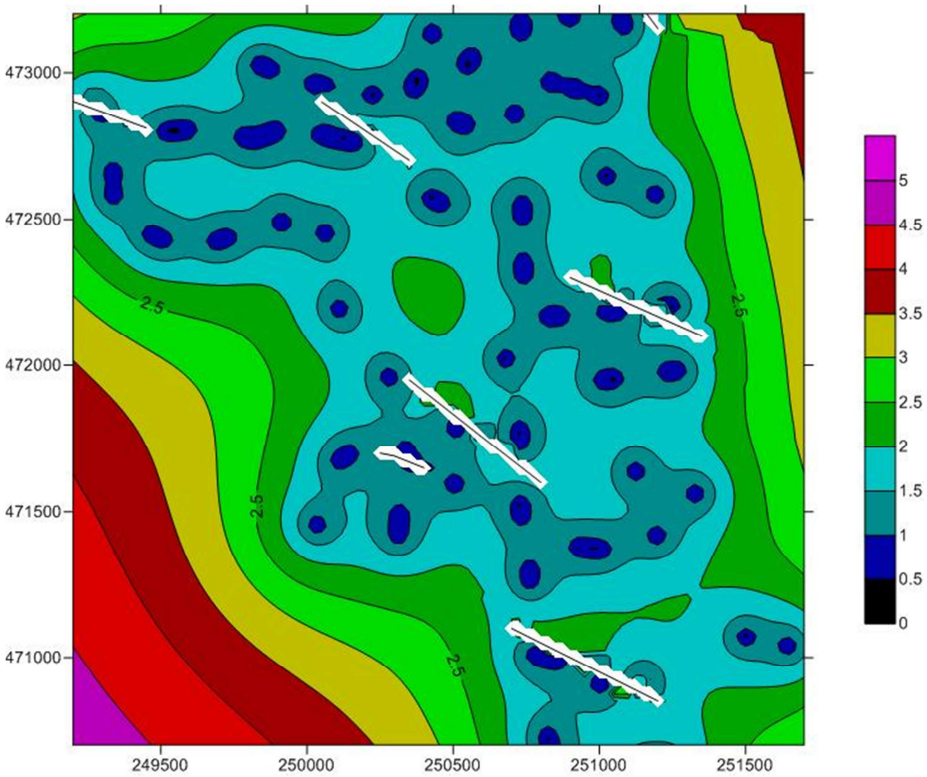

Figure 4.9 Base Tertiary uncertainty map, displayed is the standard deviation σ (in meters), which is defined as the square root of the Kriging variance.

5. The JORC Code

Using the modified Kriging method outlined in the previous chapters, an estimate of the amount of salt in place can be made. However, for such an estimate to be accepted by a stock exchange, certain international standards must be adhered to. As the JORC Code[10,11,12] is widely recognized as the standard for reporting of reserves, and is used by the Amsterdam Stock Exchange that AkzoNobel is listed on, it was opted to adhere to this code.

The JORC Code

The Australasian Joint Ore Reserves Committee (JORC) first published The Code on Reporting Mineral Resources and Ore Reserves in 1989 as a means to standardize resource and reserve reporting, which until then had seen several cases of unacceptable reporting practices[10]. The latest version was released in 2004. Over the years it has been the inspiration for most Resource and Reserve reporting standards worldwide. Most stock exchanges require companies to report their Mineral Resource and Ore Reserves according to the JORC Code or a similar standard.[11]

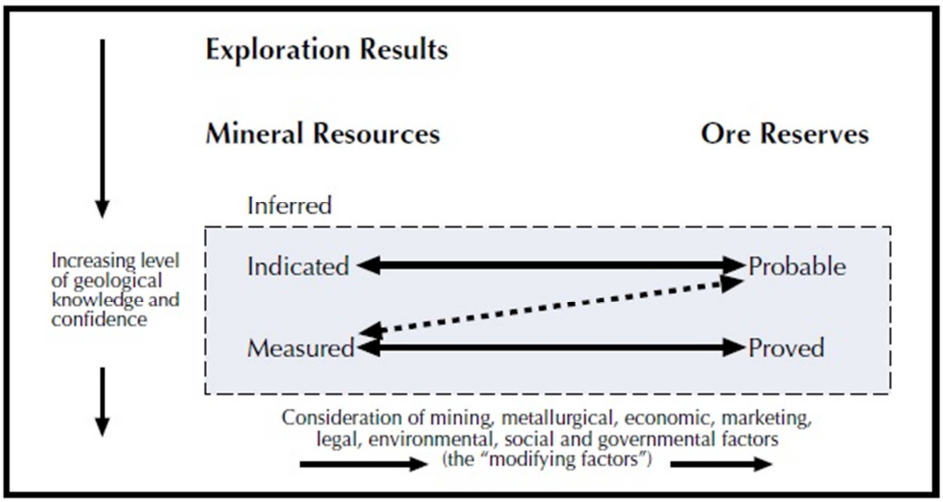

Figure 5.1: relationships between Mineral Resources and Ore Reserves. (From The JORC Code, 2004)

The JORC Code differentiates between Mineral Resources and Ore Reserves. A Mineral Resource is, as the code puts it: "a concentration or occurrence of material of intrinsic economic interest in or on the Earth's crust in such form, quality and quantity that there are reasonable prospects for eventual economic extraction."[12] Whereas an Ore Reserve is only that part of a Mineral Resource that is deemed economically mineable after all so-called 'Modifying Factors' have been considered. These Modifying Factors are mining, metallurgical, economic, marketing, legal, environmental, social and governmental factors[12]. Note that 'Ore Reserve' can be replaced with 'Coal Reserve' or 'Salt Reserve' as the situation requires[12].

The Code then divides Mineral Resources into three, and Ore Reserves into two categories. Mineral Resources can be -in order of geological confidence- Inferred, Indicated or Measured. Ore Reserves are divided in Probable and Proved Ore Reserves. Probable Reserves are the economically mineable part of an Indicated Resource; Proved Reserves are that of a Measured

Resource. Measured Resources can sometimes result in Probable Reserves. Figure 5.1 gives an overview of the system.

The code in general is very vague about what limits should be used to distinguish the various classifications. Instead, the code insists that every situation is different and categorizing the different Resources and Reserves and signing off on the total report should be done by a so-called Competent Person. The Competent Person should have plenty of experience reporting the mineral or ore in question, and should also be a member of a recognized professional organization with the power to suspend members.[11,12]

JORC Code applied to AkzoNobel

To apply the code to AkzoNobel's salt solution-mining operation, several definitions had to be tailored to this specific situation. The following definitions were formulated in cooperation with the AkzoNobel geologists (Albers, Den Hartogh, and Groenenberg):

- **"Mineral Resource"** is used for estimates based on geological information only
- **"Salt Reserve"** is used for estimates in which the *"modifying factors"* have been taken into account.
- **"Modifying Factors"** includes the consideration of mining, metallurgical, economic, marketing, legal, environmental, social and governmental factors. In the context of salt mining it encompasses e.g. the technical criteria for stability as set by the good salt mining practice, restrictions to mining due to surface infrastructure and environment, and economical considerations.
- ***"Mineral Resource"*** vs. ***"Salt Reserve"***: estimate for an entire exploration license area based on regional geological information only vs. sum of estimates on a cavern-by cavern basis taking into account cavern-specific considerations such as e.g. the technical guidelines for stability as set by the good salt mining practice, restrictions to mining due to surface infrastructure and environment, and economical considerations.
- **"Inferred Mineral Resource"** is an initial estimate during the prospecting phase of a new salt deposit. It is based on already existing subsurface data such as e.g. wells, seismic that were not obtained in the context of the new prospecting.
- **"Indicated Mineral Resource"** is a fairly reliable estimate based on widely-spaced seismic lines acquired as part of the exploration phase of the new salt prospect and/or existing well data. Boundaries of the prospect are based on the exploration license.
- **"Measured Mineral Resource**" is a highly reliable estimate based on seismic lines and new well data acquired as part of the exploration phase of the new salt prospect. Well data include an accurate estimate of the grade (% insoluble) of the salt deposit. In practice, a zone is defined around a well or a seismic line for which the extrapolation of the actual data is considered to be so reliable that it can be said to be "measured". A distance is used to define this zone, the value of which depends on the variation in the geology within the concession for which an estimate is made.
- **"Probable Salt Reserve"** is an estimate that is based on the indicated mineral resource, but with technical, infrastructural, environmental, and economical considerations taken into account.
- **"Proven Salt Reserve"** is an estimate that is based on the measured mineral resource, but with technical, infrastructural and economical considerations taken into account.

6. Mineral Resource Estimation

The Mineral Resource is estimated using the surfaces obtained in Chapter 4. The classification is done using both a probabilistic and a deterministic approach. The probabilistic approach involves randomizing the model we obtained and then using a Monte Carlo simulation to obtain a cumulative probability curve of the amount of salt in place. The deterministic approach is much simpler and merely involves getting the expected amount of salt based on expected values. The two obtained results are used to see if they can in any way be translated into each other.

Preparation

To correctly estimate the amount of salt in place using the surfaces from Chapter 4, these surfaces have to be treated first. For a good overview of the expected amount of salt in place, a thickness map is constructed first. This is done by simply subtracting the Base MRE depth values from the Top Salt C depth values. The result is shown in Figure 6.1.

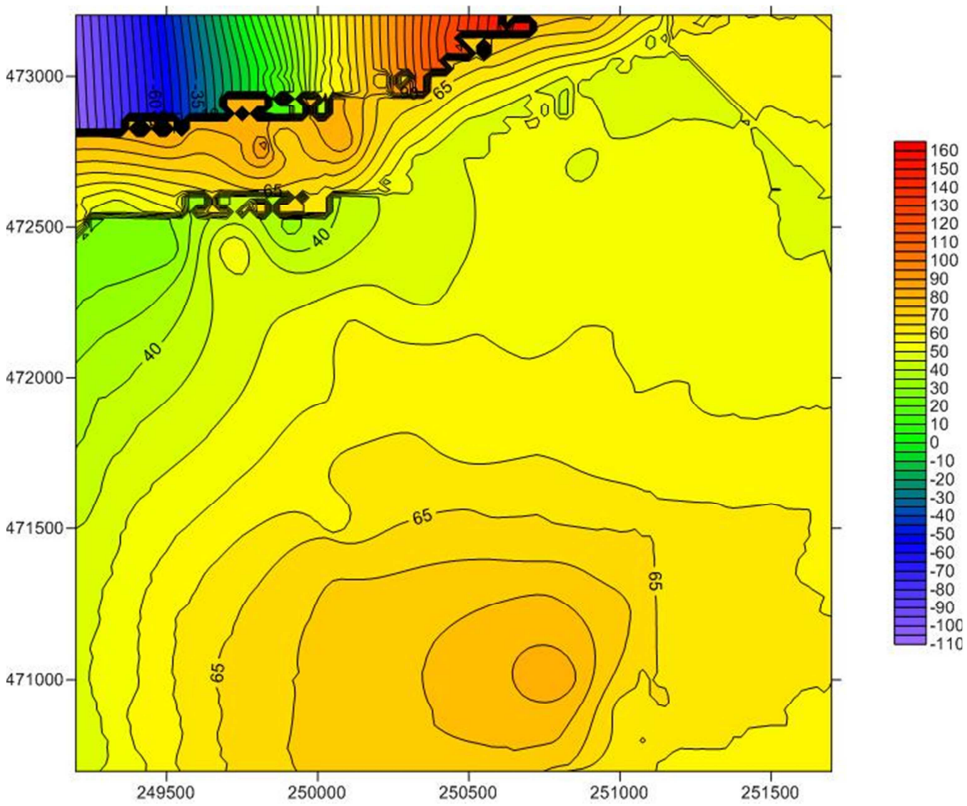

Figure 6.1 Thickness of the salt layer between Base Main Röt Evaporite and Top C

Salt D and Salt E can effectively be left out of all following calculations, because they do not have a reasonable prospect of ever being extractable due to stability (D&E) and grade (E) concerns.

Furthermore, as already discussed in Chapter 4, some areas have to be left out of the evaluation, because the Kriging process caused some artefacts in the model. Therefore the discussed areas around the faults and in the top left corner will be taken out of the model. The 'area around the faults' was chosen to be the area within 100 meters from the fault line. This is

also the area the GSMP guidelines say must never be mined from. The results are shown in Figure 6.2. The same "blanking" operation, as it is called, has been performed on the maps of the Base MRE and Top Salt C for use in the probabilistic approach.

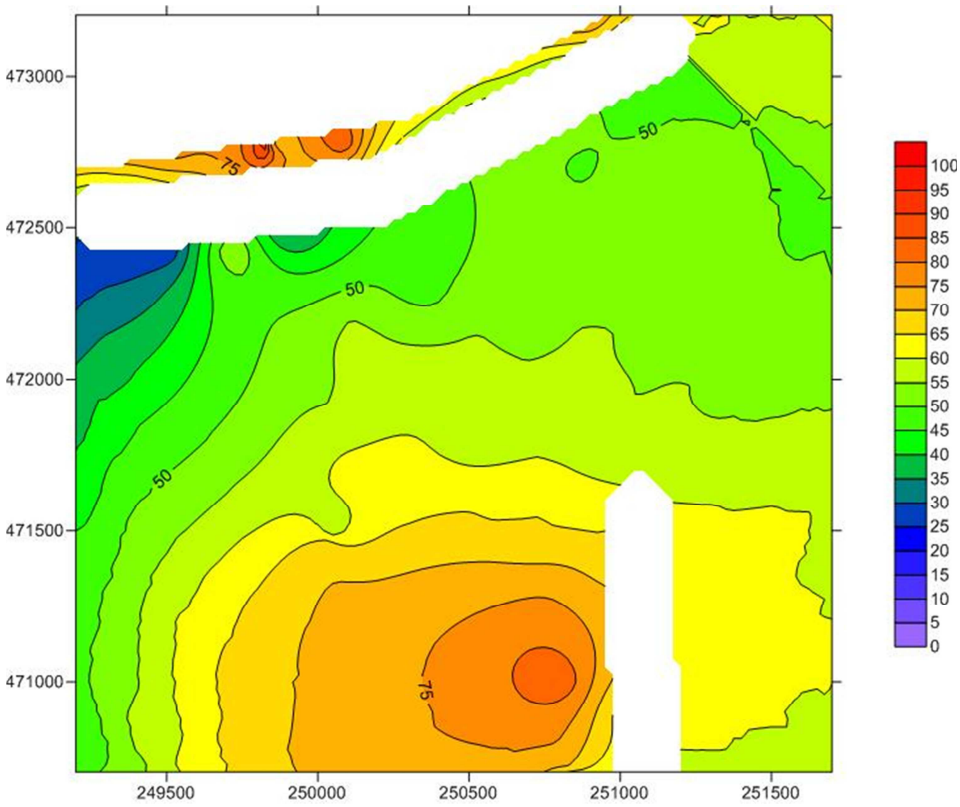

Figure 6.2 Thickness of the salt layer between Base Main Röt Evaporite and Top C with the disregarded areas 'blanked'. Please note how the contrast of the remaining areas is increased.

To further estimate the amount of salt in place, the grade of the salt body must be known. For this, the borehole data was evaluated for the thickness of the individual rock benches in the salt. For each rock bench, the average thickness as a percentage of the total salt thickness was calculated. Also the standard deviation of the measurements was taken. This allows for the simulation of the rock bench thickness at a single location. However, if those values are averaged, chances are the value we come up with is the average value we found, although this average value of the sample may not hold for the entire field. Therefore the standard deviation of the mean was also found, using (4) with *n* being the number of samples.

$$\sigma_{mean} = {}^{\sigma_{sample}}/_{\sqrt{n}} \qquad (4)$$

The results can be found in Table 1

Table 1: Fraction of non-salt layers in the salt between Base MRE and Top Salt C and related standard deviations

	Rock A	Rock B	Rock C
Mean	0.0072	0.018	0.036
σ	0.0082	0.0075	0.012
σ_{mean}	0.0026	0.0012	0.0018

To further increase the confidence of the Mineral Resource estimation, an estimate of the amount of insoluble contents in the salt layers is required. Unfortunately there were no measurements into this aspect available at the time of research, so a rule of thumb estimate of 10% was used.

Probabilistic approach

For the probabilistic approach a Monte Carlo simulation is set-up, using the depth values and standard deviations obtained in Chapter 4, as well as the mean rock grade and the standard deviation of this mean. For every iterative simulation, the 'blanked' surfaces of the Base MRE and the Top Salt C are recalculated using a normally distributed random number for each surface and their related uncertainties. From this the simulated thickness is acquired by subtracting the depth of the Base MRE from the depth of the Top Salt C. The total rock bench percentage is calculated using the mean and σ_{mean} values from Table 1 and three normally distributed random numbers. The complement of this value (1-value) times the thickness of the salt body then gives the net salt column per grid block. This is then multiplied with 90% (10% insoluble material assumed) to give the actual salt content in the column. Then the height of the column is converted into m^3 and then into tons of mass using a salt density of 2165 kg/m^3. The resulting curve is shown in Figure 6.3.

From this curve several things can be seen. The point of 50% probability – called the P50 value – indicates the expected value of the total Mineral Resource. This value can also be found using the deterministic approach, because in that approach only expected values are used, leading to the expected result. The steepness of the curve tells something about the uncertainty. The steeper the curve, the more the values are close to each other, so it is more likely that the expected value is indeed the real value. This means less risk. On the other hand, a greater spread in values might also indicate that there is a lot more resources actually present. The risk is higher but the profits are potentially bigger. To quantify the steepness of the curve, two more values are needed. Usually the so-called P10 and P90 values are taken[1]. These are the values at respectively 10% and 90% cumulative probability. The three values, P10, P50 and P90 are given in Table 2, as well as P90 divided by P10 as a single number to quantify the slope steepness.

Table 2: The P10, P50 and P90 values of the cumulative probability curves for the Salt In Place (SIP), all masses in Mt.

	Total	<500m	GeoWulf area
P10	415	340	228
P50	552	435	278
P90	703	525	328
P90/P10	1.69	1.54	1.44

[1] In this report, P(n) is the value for which the chance of the value being smaller than this value is (n)%.

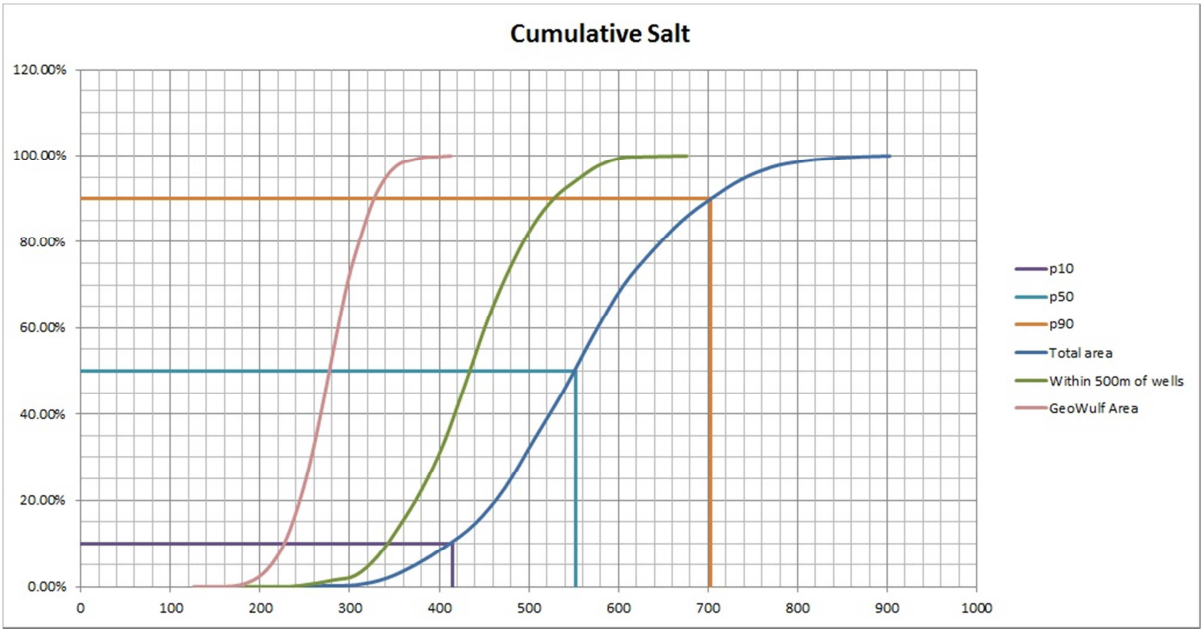

Figure 6.3: cumulative probability distributions for the Salt In Place (SIP) for the three scenarios. The p10, p50 and p90 have also been indicated.

Deterministic approach

For the deterministic approach, the values of the blanked thickness map (Figure 6.2) are multiplied with the inverse rock bench grades then again with 90% to get the salt column. The salt column is then converted to salt mass in the same way as was done for the probabilistic approach.

In this way, however, uncertainty is not included. For this the definitions of Chapter 5 are used. As each situation calls for a separate evaluation of the area that can be used as a basis for a Measured Resource estimation, two example boundaries are used to show the effect of changing this distance. Those two boundaries are: (1) the area within a distance of 500m from the nearest measurement, and (2) the area which has been correlated by GeoWulf. This last area is effectively the area enclosed within the boreholes. The thickness map of Figure 6.2 has again been blanked to show only the thicknesses within those boundaries, producing figures 6.4 and 6.5. A value of 500m has been chosen for the distance of the first boundary, because it is reasonable to assume that the geology will be continuous for another 500m from this area. The results of the calculations can be found in Table 3.

Table 3: Determined Salt in place for the three scenarios

Area	Salt in place	
Total	552	Mt
<500m	435	Mt
GeoWulf area	278	Mt

Because the algorithm for the probabilistic approach was already constructed, it was decided to run it for the two other scenarios as well, hoping for it to give more insight in the relation between the two approaches. The results are also plotted in Figure 6.3; the P10, P50 and P90 values are given in Table 2.

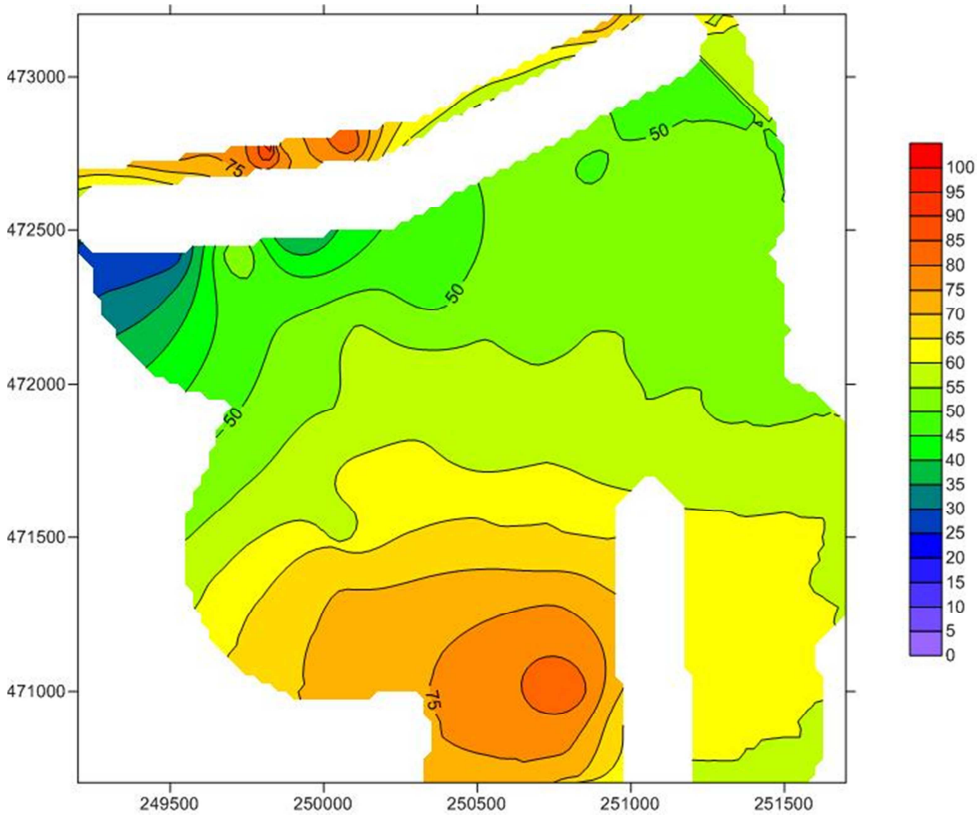

Figure 6.4: the thickness map of the area within 500m of a borehole.

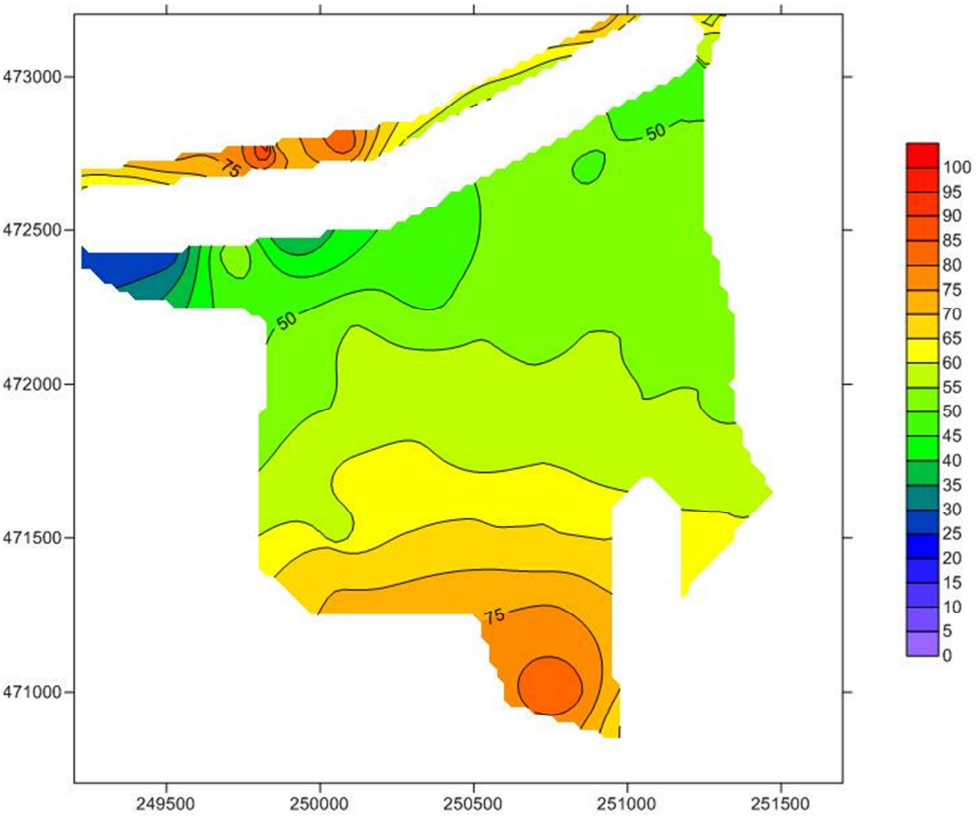

Figure 6.5: the thickness map of the area examined by GeoWulf.

Discussion

The thickness map (Figure 6.1) shows some unnatural behavior in the top right corner. This is probably related to the fault line running nearby and therefore an artefact of the modeling process. Because it is in an area that is of no significance it will not be looked at any further. However, it is recommended for future projects that this artifact be further investigated by for instance defining a hypothetical fault line that runs to the edge of the map.

When comparing the determined values and the p50 values of the three areas, it becomes obvious that these must have the same meaning. This is also logical from a statistical point of view, as the random variables in the Monte Carlo simulation are unrelated and therefore the expected result of the simulation will be same as the result of the simulation with expected values.

It is of course obvious that as the area is tightened around the boreholes, the model becomes more certain –i.e. the probability curves of the scenarios steepen and the p50 values go down.

The p10 value indicates that there is 10% chance that there will be less salt in the studied area than that corresponding to the P10 value. The same holds for the P90 and 90%. It could therefore be that the P10 value is a Measured Mineral Resource, as we are very confident that at least this amount of salt is present in the subsurface. In the same way we can argue that the P50 corresponds to an Indicated Mineral Resource and P90 to an Inferred Mineral Resource. If we want to translate these values to the deterministic approach, we find that the obtained value for the area within a distance of 500m from the wells corresponds to roughly the P10 value of the entire area. It would be interesting to see if this holds for larger areas, that contain the same data density, as well. As it is, this being a single case, it can also be coincidence.

What is more acceptable is the idea of putting forward the actually measured and correlated data as the basis for a Measured Resource –i.e. taking the determined value of the Geowulf area as Measured. This differs from earlier definitions in that seismic data may aid in this, but is not absolutely necessary. The area within, in this case, 500m can then be used as a basis for calculating the Indicated Resource. Again, this 500m boundary is only valid for this case. Each area has to be examined for large tectonic structures before such numbers can be defined. As a basis for Inferred Resources, the total area can be used. It is up to the Competent Person to decide on using the P50 or the P90 value for the Inferred Resource. It would be advisable to always use the P50 for this, so as to not overestimate the Resource.

It appears that the values estimated using a deterministic approach (and then also the P50 values of the probabilistic approach) are the most valuable ones when it comes to giving a single number. However, it is important to realize that there are uncertainties connected to these values. The P10 and P90 values can then be used to quantify this uncertainty preferably by dividing P90 by P10. The higher this value, the more gradual the slope of the cumulative probability plots, and thus the higher the uncertainty.

The Measured Mineral Resource is 278 Mt with slope 1.44, with an additional 159 Mt of Indicated Mineral Resource with slope 1.76 and an Inferred Mineral Resource of 117 Mt with slope 2.37. Please note that these numbers do not account for salt that is already produced. If this were taken into account, the Measured Resource would dramatically fall, because this is the area in which production has already taken place to a point where the reserve is depleted. The other figures would remain unchanged, as no salt production has taken place in the areas outside of the ‘measured’ area.

7. Salt Reserve

Now that the Mineral Resource has been estimated, the Modifying Factors can be used to estimate the Salt Reserve. Since the data on the Modifying Factors in the Hengelo area are limited, and time was scarce, the following chapter will only give a short overview of the estimation steps. The main focus will lie with Modifying Factors presented by the mining method.

Maximum cavern height

To first get an overview on which areas may be best suitable for development, a map of the maximum cavern height is constructed. This is done using formulae (1) and (2) presented in Chapter 3 in conjunction with the maps constructed in Chapter 4. The smallest outcome of these two calculations will be taken as the TCAV or top of the cavern. The TCAV is then used in conjunction with the BCAV –bottom of the cavern – to give the HCAV – maximum cavern height. The BCAV is a function of both the Base of the MRE and the amount of rock in the salt body, as this will fall to the bottom of the cavern during production. The amount of rock is calculated in the same way as in Chapter 6, deterministically. An additional 0.5m of salt is assumed to be left in the base of the cavern, to prevent against leaking of brine to lower strata. This means that the BCAV can be calculated using (6).

$$\text{BCAV} = \text{Base MRE} + 0.5 + \Sigma \text{ rock benches} \qquad (6)$$

The resulting HCAV map is presented in Figure 7.1.

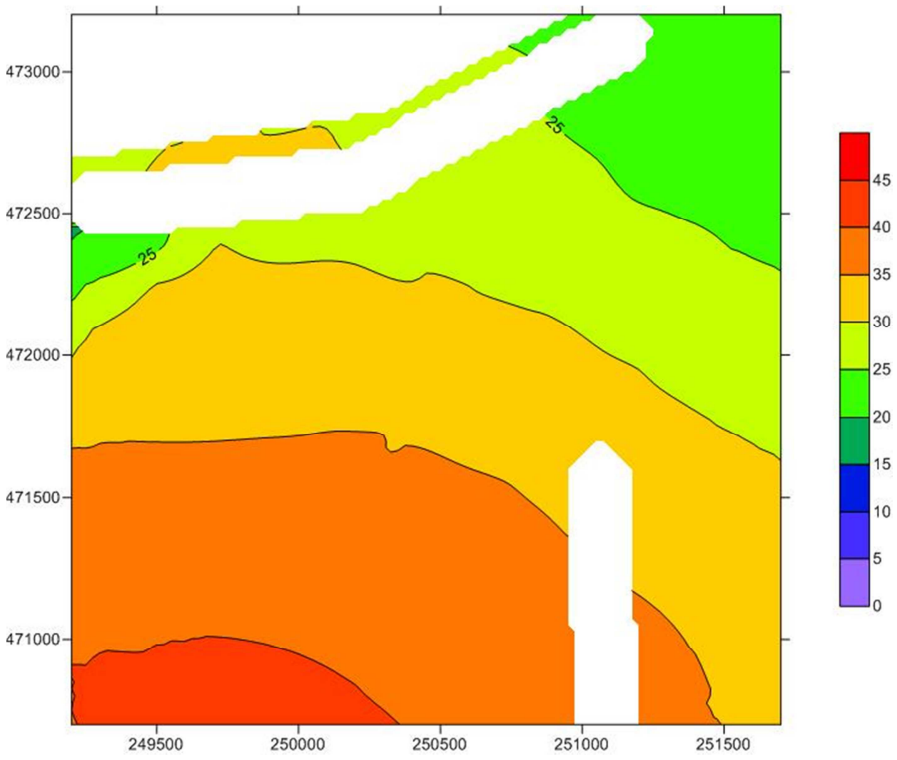

Figure 7.1: maximum cavern height in the area

Reserve per cavern

To be able to quickly calculate the total reserve in different scenarios, it is important to know the amount of salt that can be produced from a cavern. Since the HCAV is now known throughout the area, it is a good idea to make the amount a function of HCAV. The geometry of an SSC cavern can be seen to be the combination of two different geometrical shapes; a cone that represents the sump and a cylinder that represents the production phase of the cavern. The cone has a diameter of 80m, the cylinder a diameter of 120m. The shape of the cone allows for a slight correction of the BCAV[1], due to the difference in bottom depth along the cavern. All-in-all this leads to (7) for the volume per cavern (VCAV) in m^3.

$$VCAV = 4188.79 + 11309.73 * (HCAV - 2.1875) \quad (7)$$

The volume of the cavern then has to be translated into a mass of mineable salt. Here again the assumed 10% of insoluble content is subtracted to come to the volume of mineable salt. However, for every m^3 of salt extracted, 1 m^3 of brine is left behind. This means that for every m^3 of mineable salt there is 2.165 – 0.312 (density of pure salt – salt mass in brine) = 1.853 tons of salt actually produced.

Cavern placement

Finally, a design of the cavern placement in the area can be made. Several factors have to be taken into account when doing this. First of all, in Chapter 3 some parameters were given for the lay-out of a cavern grid, specifying that caverns should be placed 150m apart in rows that lay 450m apart. Secondly, in areas that are not suited for production, there should be no caverns planned. This could be areas where the maximum cavern height falls below an economic boundary, where the surface is urbanized, is part of a nature reserve or is otherwise unfavorable for mining operations.

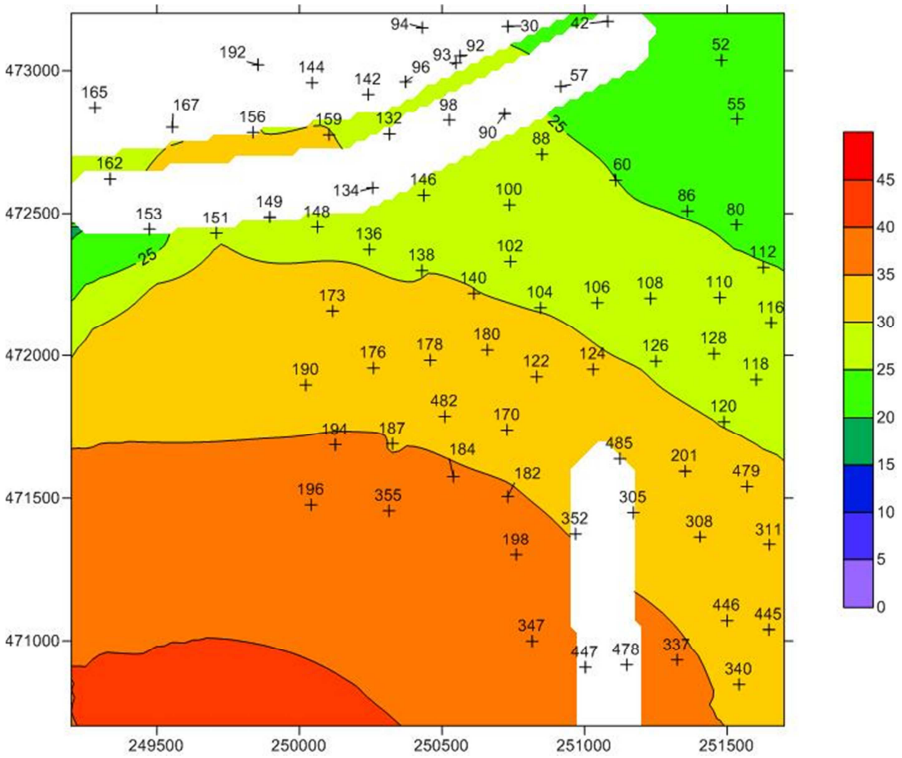

Figure 7.2: cavern lay-out as selected for scenario 1, each number corresponds to that of an actual borehole at the same location.

As an example, three scenarios have been worked out:

1. Salt has been produced in this area in the past, using outdated cavern designs. What would be the Salt Produced if the same locations had been chosen to produce salt using the modern SCC design? And what would be the historical recovery?
2. Assuming no production had taken place in the past, what would be the total Salt Reserve when developing the field according to current best practices?
3. What is the Salt Reserve left in the area?

The three scenarios lead to three cavern lay-outs as presented in figures 7.2, 7.3 and 7.4. Note that in all three cases, urbanization or other unfavorable conditions at surface level have been left out of consideration.

Results

For Scenario 1, 25 caverns were found to be situated outside of the examined areas. Because we want to know the recovery of a complete cavern, caverns still in production were also not examined, leaving 5 out. This leaves 45 caverns that were examined. The total historical production was 23.2 Mt. The total theoretical modern production is 29.1 Mt. This gives a recovery of 79.8%. However, this percentage varies wildly from cavern to cavern, and is not considered an accurate predictor for single caverns.

For Scenario 2, out of the 96 caverns placed in a grid, 24 were found to be outside of the examined areas. The other 72 were found to contain 62.8 Mt of salt.

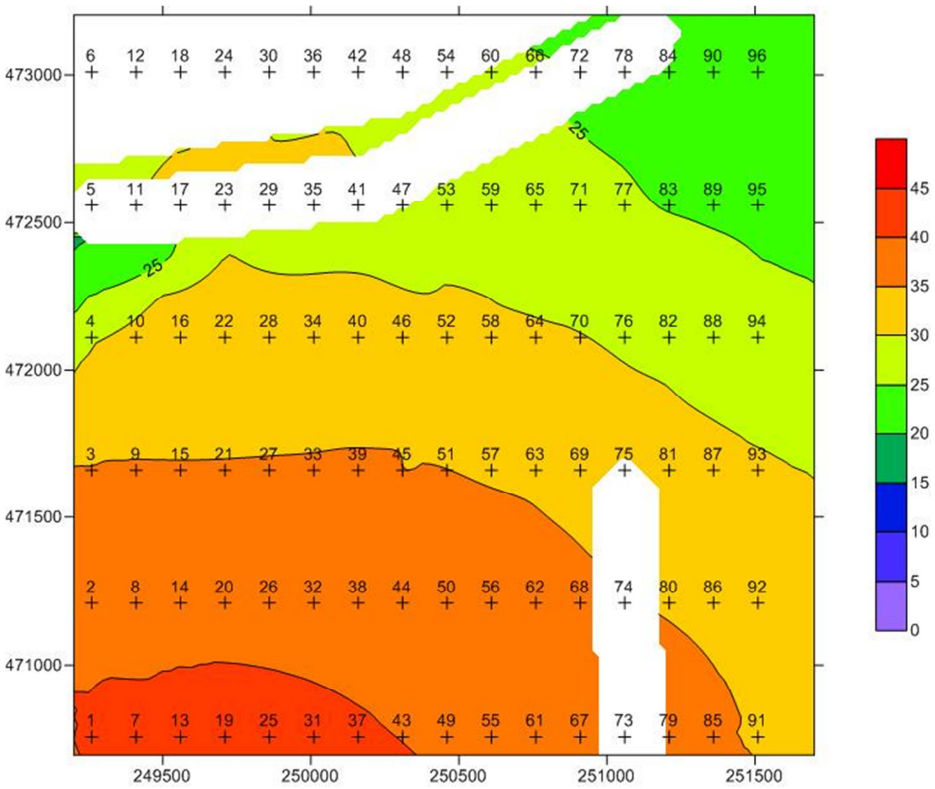

Figure 7.3: cavern lay-out as selected for Scenario 2.

For Scenario 3, the 5 caverns that were left out of Scenario 1 were taken into account again, as they *are* of the SSC type, and therefore remaining production could be predicted (estimated to be 3.8 Mt). It was found that 30 more new caverns could be developed containing a total reserve of 24.2 Mt. This leads to a value for total remaining reserves of 28.0 Mt. As this scenario is most important and most diverse, it is interesting to classify these results according to the JORC Code. The only caverns situated within the Geowulf area are the ones still producing. We can therefore safely say that the Proved Salt Reserve is 3.8 Mt. Of the other caverns, the numbers 1, 2, 3, 4, 7, 8, 9, 13, 19, 25, 31, 37 and 43 fall outside of the 500m boundary that was set for the Indicated Mineral Resource. These are therefore considered to be an Inferred Resource, and will not be treated as a Reserve. This means that the Probable Reserves are 13.6 Mt.

Note that the lay-out presented in scenarios 2 and 3 may not be ideal for maximum production. Figures stated are considered to be minimal values.

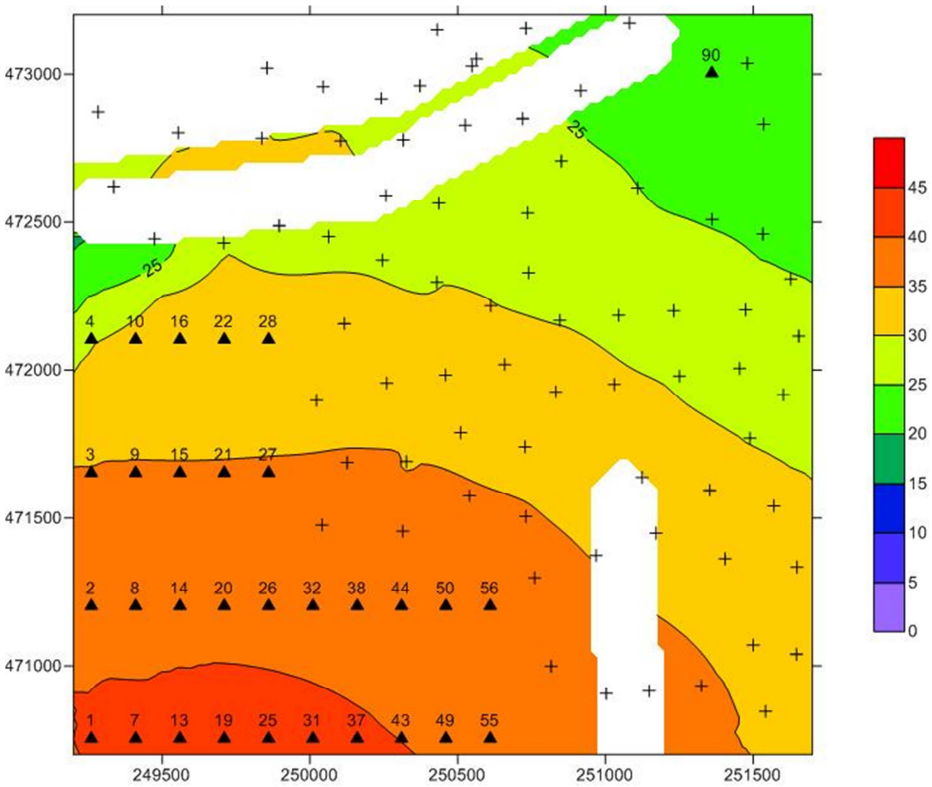

Figure 7.4: cavern lay-out as selected for Scenario 3. Please note that this is in fact a combination of scenarios 1 & 2.

8. Conclusions & Recommendations

It can be concluded that:

- Kriging as an interpolation technique is of limited use when limited data, or unevenly spread data is available.
- The added bonus of uncertainty values provided by Kriging is of limited use in calculating the Mineral Resource of a bedded salt deposit.
- The definitions of the JORC Code as translated to the AkzoNobel leaching operation are adequate for all scenarios presented.
- Resources should be classified on the basis of geological certainty, with numerical uncertainty used to give a confidence level to the value associated with that geologic certainty. As every estimate will have certain uncertainty, it is best to quantify this as much as possible.
- Estimating a recovery factor for existing caverns was implausible, because the caverns in the area were either from well before GSMP times, or are still in production.

The results of the estimation and categorization of Resources and Reserves are listed in Table 4. As these have been categorized conservatively, they should be treated as indicative.

Table 4: Outcome of evaluation of the area under consideration

Mineral Resource		Resource Uncertainty	Salt Reserve	
Inferred	117 Mt	1.44	-	-
Indicated	159 Mt	1.76	Probable	13.6 Mt
Measured	3.8 Mt	2.37	Proven	3.8 Mt

Further, it is recommended that:

- Seismic data be included in further studies, as this could pose new questions regarding the definitions defined in Chapter 5. Also, it will enhance the understanding of the subsurface.
- Future exploration be done with the aim of achieving an even spread of data points throughout the target area. This will result in the Resources and Reserves being categorized in a category of higher certainty, and thus higher value.
- Data analysis after exploration is focussed toward finding discontinuities, as these are the main features affecting the otherwise very consistent bedded salt.
- The data is processed using (a) less demanding interpolation technique(s) than Kriging, as the added bonuses of Kriging are negligible and the process may possibly produce a less realistic model than others.
- The actual reserves contained within caverns of various sizes are calculated, and used for future estimations.
- Further research is done into the various Modifying Factors affecting the mining of salt, such as economic and processing factors.
- AkzoNobel requires someone who is internationally recognized as a Competent Person in the area of salt mining, meaning they have to fulfil all the requirements as stated in the JORC Code, to be able to submit reserves as assets.

References

[1] Geluk, M.C.;Triassic, in Geology of the Netherlands p85-106, Royal Netherlands Academy of Arts and Sciences, 2007

[2] Geluk, M.C.; Stratigraphy and tectonics of Permo-Triassic basins in the Netherlands and surrounding areas, 2007, http://home.kpn.nl/mark.geluk/Map16.htm

[3] Wong, Th.E.; Jurassic, in Geology of the Netherlands p107-125, Royal Netherlands Academy of Arts and Sciences, 2007

[4] GEOWULF Laboratories, Geological Framework TWR Area, Compilation Report project number GL08.502, 2008

[5] GEOWULF Laboratories, Detailed Geology of the Hengelo Solution Mining Area, Part 1 (Draft) , project number GL10.101, 2010

[6] AkzoNobel, Hengelo Uitloog Techniek (HUT), 6e actualisering, 2011

[7] Van Lange, M.W.P.; The Development, Geology and Lithology of the Central-Northern Part of the Hengelo Rock Salt Solution Mining Area and its Geotechnical Characterisation (+ Appendix). Memoirs of the Center of Engineering Geology in the Netherlands, No. 126, Technical University Delft, Faculty of Mining and Petroleum Engineering, Section Engineering Geology, Delft, December 1994.

[8] Isaaks E.H. & Mohan Srivastava, R; An Introdution to Applied Geostatistics, Oxford University Press, 1989

[9] Swan, A.R.H. & Sandilands, M.; Introduction to Geological Data Analysis, Blackwell Science, 1995

[10] JORC, History of the JORC Code, www.jorc.org/history.asp

[11] Larkin, D.; What is the JORC Code?, Press release of The Australasian Institute of Mining & Metallurgy, http://jorc.org/pdf/whatisthejorccode.pdf

[12] JORC, The JORC Code 2004, http://jorc.org/pdf/jorc2004print_v2.pdf

Also, for an understanding of how reserves have been reported in the past, the author read:

TNO-NITG, Kartering Twenthe-Rijn, Uitbreiding Twenthe-Rijn en Buurse Concessie, projectnummer 147377611,Haarlem, april 1997.

TNO-NITG, Actualisering van de bestaande geologische kaarten van de concessie Adolf van Nassau en van de concessies Twenthe-Rijn, Buurse en Uitbreiding Twenthe-Rijn, projectnummer NITG 02-194-C, Utrecht, december 2002.

Oranjewoud N.V., Reserveberekening winningsvergunningen, Twenthe-Rijn en Twenthe-Rijn Uitbreiding (boorterrein Hengelo), projectnummer 64872-36, 2003

MWH B.V., Salt mining possibilities in areas adjacent to the Hengelo brine field, final report, project number W09B0028, 2010

The cover image comes from the collection of the Mining Technology Department of AkzoNobel.

Appendix 2
Variogram parameters and used sample variograms

	Layer	Model*	Drift	Range	Sill	Nugget	lag size**	# wells
1	Base MRE	1	1	1500	225	0	15	197
2	Top A	1	1	1800	300	0	25	48
3	Base A	1	1	1500	300	0	3	15
4	Top B	1	1	1800	250	0	50	49
5	Base B	1	1	2000	300	0	25	45
6	Top C	1	1	2200	250	0	25	68
7	Base C	1	1	1900	260	0	25	49
8	Top D	1	1	2800	250	0	25	51
9	Base D	1	1	2800	250	0	25	51
10	Top E	2	1	3200	500	0	50	131
11	Base E	2	1	3200	500	0	50	139
13	Base Tertiary	2	1	1500	28	0	50	164

*Model

1 Circular
2 Exponential
3 Linear

**lags are blocks on the distance axis over which the value in that block are averaged
this is to create a smoother line, and reduce the number of data points

Sample Variogram of Base MRE

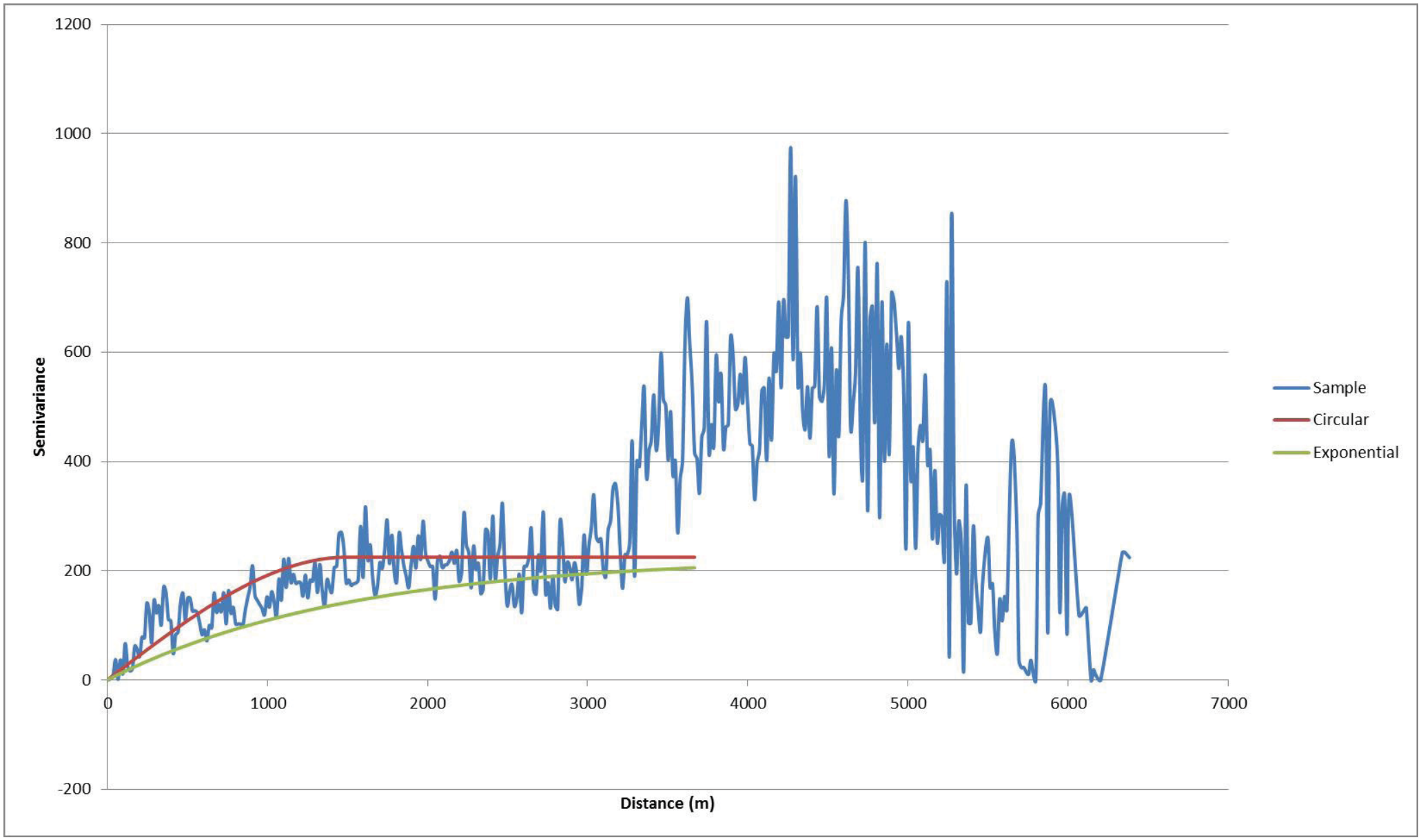

Sample Variogram of Top Salt C

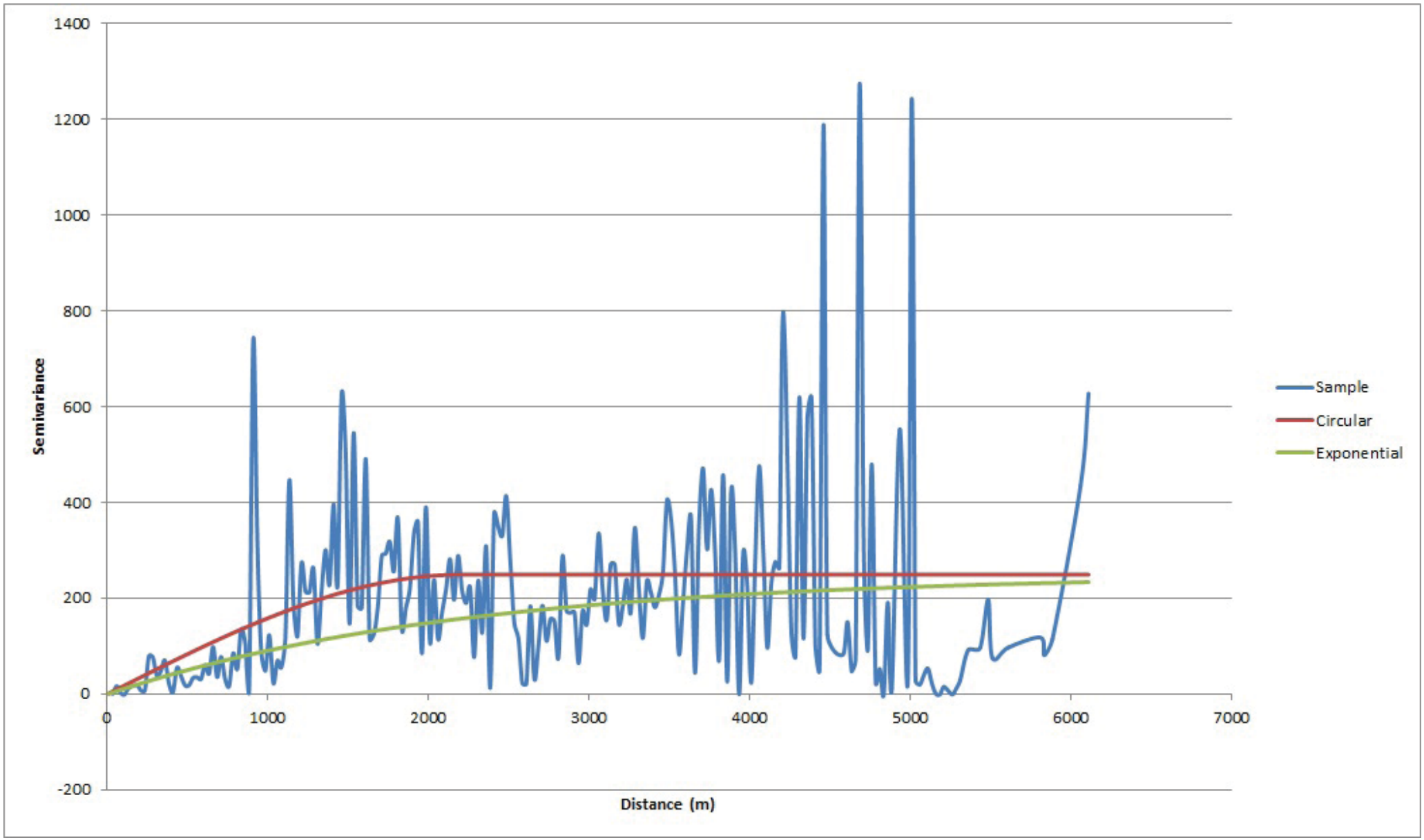

Sample Variogram of Base Tertiary